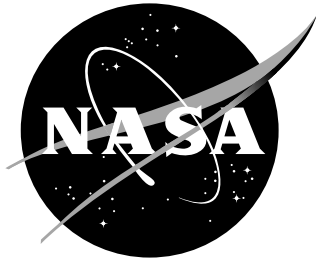


NASA/CR-2002-211746



NWRA AVOSS Wake Vortex Prediction Algorithm Version 3.1.1

*R. E. Robins and D. P. Delisi
Northwest Research Associates, Inc.
Bellevue, Washington*

June 2002

The NASA STI Program Office ... in Profile

Since its founding, NASA has been dedicated to the advancement of aeronautics and space science. The NASA Scientific and Technical Information (STI) Program Office plays a key part in helping NASA maintain this important role.

The NASA STI Program Office is operated by Langley Research Center, the lead center for NASA's scientific and technical information. The NASA STI Program Office provides access to the NASA STI Database, the largest collection of aeronautical and space science STI in the world. The Program Office is also NASA's institutional mechanism for disseminating the results of its research and development activities. These results are published by NASA in the NASA STI Report Series, which includes the following report types:

- **TECHNICAL PUBLICATION.** Reports of completed research or a major significant phase of research that present the results of NASA programs and include extensive data or theoretical analysis. Includes compilations of significant scientific and technical data and information deemed to be of continuing reference value. NASA counterpart of peer-reviewed formal professional papers, but having less stringent limitations on manuscript length and extent of graphic presentations.
- **TECHNICAL MEMORANDUM.** Scientific and technical findings that are preliminary or of specialized interest, e.g., quick release reports, working papers, and bibliographies that contain minimal annotation. Does not contain extensive analysis.
- **CONTRACTOR REPORT.** Scientific and technical findings by NASA-sponsored contractors and grantees.

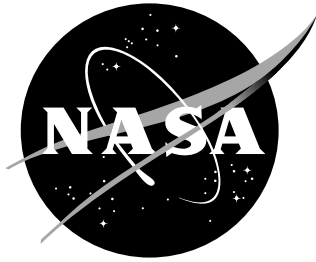
- **CONFERENCE PUBLICATION.** Collected papers from scientific and technical conferences, symposia, seminars, or other meetings sponsored or co-sponsored by NASA.
- **SPECIAL PUBLICATION.** Scientific, technical, or historical information from NASA programs, projects, and missions, often concerned with subjects having substantial public interest.
- **TECHNICAL TRANSLATION.** English-language translations of foreign scientific and technical material pertinent to NASA's mission.

Specialized services that complement the STI Program Office's diverse offerings include creating custom thesauri, building customized databases, organizing and publishing research results ... even providing videos.

For more information about the NASA STI Program Office, see the following:

- Access the NASA STI Program Home Page at <http://www.sti.nasa.gov>
- E-mail your question via the Internet to help@sti.nasa.gov
- Fax your question to the NASA STI Help Desk at (301) 621-0134
- Phone the NASA STI Help Desk at (301) 621-0390
- Write to:
NASA STI Help Desk
NASA Center for AeroSpace Information
7121 Standard Drive
Hanover, MD 21076-1320

NASA/CR-2002-211746



NWRA AVOSS Wake Vortex Prediction Algorithm Version 3.1.1

*R. E. Robins and D. P. Delisi
Northwest Research Associates, Inc.
Bellevue, Washington*

National Aeronautics and
Space Administration

Langley Research Center
Hampton, Virginia 23681-2199

Prepared for Langley Research Center
under Contract NAS1-99074

June 2002

Available from:

NASA Center for AeroSpace Information (CASI)
7121 Standard Drive
Hanover, MD 21076-1320
(301) 621-0390

National Technical Information Service (NTIS)
5285 Port Royal Road
Springfield, VA 22161-2171
(703) 605-6000

Table of Contents

Abstract.....	ii
1. Introduction.....	1
2. Background	2
3. Algorithm Description.....	3
3.1 EDR Version of Phase I.....	4
3.2 Phase II.....	6
3.3 Phase III.....	7
3.4 Phase IV	8
4. Logic Description	10
5. Implementation Details.....	11
5.1 Running the Algorithm.	11
5.2 Source Code Organization.	12
Acknowledgements	14
References.....	14
Figures.....	15
Appendix A. TKE Version of Phase I.....	A-1
Appendix B. Corrections for Time to Leave Corridor.....	B-1
Appendix C. Circulation Decay Model for Ground Interaction	C-1
Appendix D. Description of APA.OUT.....	D-1
Appendix E. Sample Algorithm Driver	E-1
Appendix F. Test Cases	F-1
Appendix G. Supplementary Charts.....	G-1

Abstract

This report provides a detailed description of the wake vortex prediction algorithm used in the Demonstration Version of NASA's Aircraft Vortex Spacing System (AVOSS). The report includes all equations used in the algorithm, an explanation of how to run the algorithm, and a discussion of how the source code for the algorithm is organized. Several appendices contain important supplementary information, including suggestions for enhancing the algorithm and results from test cases.

1. Introduction

An important component of the Aircraft Vortex Spacing System (AVOSS) being developed at NASA's Langley Research Center (LaRC) is an algorithm that can estimate the length of time that trailing vortices may remain a hazard for any aircraft flying towards them. Northwest Research Associates, Inc. (NWRA), in association with Prof. T. Sarpkaya of the Naval Postgraduate School and F.H. Proctor of NASA's LaRC, and with support from the AVOSS group at LaRC, headed by D.A. Hinton, has contributed to the formulation of this component by developing, validating and implementing an algorithm that predicts the trajectories and circulation decay of trailing vortices.

A critical requirement of the algorithm is that it must execute fast enough (about 0.1 sec per case on state-of-the-art workstations) to be run by AVOSS several hundred times during the first few minutes of every half-hour. The reason for such a large number of executions is that the algorithm must be run for a number of atmospheric profiles (based on deviations from measured profiles) and numerous aircraft types to provide estimates of how long it may take trailing vortices to either move out of the flight corridor of any given oncoming aircraft or to decay to a non-hazardous level of intensity (definition of AVOSS flight corridors is given by Hinton [1996]). AVOSS then uses these estimates to define aircraft separation matrices that may result in increased airport capacity. The algorithm, originally coded in FORTRAN, has been converted to C++ with the help of personnel from Research Triangle Institute and Computer Sciences Corporation.

A summary of the algorithm's evolution is as follows. The original FORTRAN version, completed December 1997, was called Version 1. This version was converted to C++ for incorporation into AVOSS. Improvements were made to this version for vortices generated near the ground and the resulting version, called Version 2, was brought under configuration control in April 1999. A new version, which used an eddy dissipation rate model (instead of a turbulent kinetic energy model) for the effects of atmospheric turbulence, was brought under configuration control in August 1999 and was called Version 3. Improvements to prevent premature termination of the algorithm were made in September 1999, the result being Version 3.1. A minor bug was fixed in March 2000, resulting in the AVOSS version, called Version 3.1.1. Finally, a new circulation decay model for vortices interacting with the ground was added in September 2000 (see Appendix C); this version, called Version 3.2, is currently undergoing evaluation.

The following sections describe the AVOSS demonstration version (Version 3.1.1) of the NWRA AVOSS Prediction Algorithm (APA). Section 2 discusses previous studies of wake vortex algorithm development, Section 3 contains a detailed discussion of the equations that the algorithm solves, Section 4 presents the flow of logic in the algorithm, and Section 5 provides information on implementing and running the code. Several appendices augment the discussions in these sections. Information on the algorithm's performance is available in a report by Robins and Delisi (2002).

2. Background

Previous studies aimed at the development of an operationally useful wake vortex prediction algorithm were reported by Greene (1986), Liu (1991), and Corjon and Poinot (1996). Greene considered the effects of stratification, turbulence and viscous damping on the descent of trailing vortices. His approach was heuristic and resulted in an ordinary differential equation to describe the descent of the vortices. The atmospheric stratifications assumed by Greene corresponded to buoyancy forces that were linear functions of the vortices' descent distance. Greene did not consider cross winds or ground effects.

Liu focused on a model for the effects of secondary vorticity generated by interaction between the ground and the descending vortices. Liu's approach was to introduce secondary vortices having circulation of sign opposite to that of the primary vortices. He used laboratory results to guide his choice for the initial location and magnitude of the secondary vortices, and did not allow any of the vortex strengths to vary. He constrained each secondary vortex to be a fixed distance from the primary vortex responsible for its generation, and did not employ secondary image vortices to satisfy the condition of zero vertical velocity at the ground. In addition, Liu considered the effect of secondary vorticity on the primary vortices only until the secondary vortices had rotated part way around the primary vortices. He did not consider longer-term effects of the secondary vorticity or the further generation of secondary vorticity.

Corjon and Poinot added cross wind to Liu's model, allowed the primary and secondary vorticity to vary, as long as the ratio between the two remained fixed, and included a term for the decay of the downwind vortex due to shear effects. As with Liu, they did not include secondary image vortices to ensure that the vertical velocity at the ground be zero.

Although the above efforts resulted in valuable insights, they each treated just a portion of the vortices' evolution. Thus, these efforts did not result in an algorithm that could compute the evolution of trailing vortices in a realistic atmosphere from the time of generation through the sustained interaction of the vortices with the ground. The NWRA algorithm has combined and extended these previous efforts in such a way that it is able to compute the entire evolution of the vortices in a realistic environment.

3. Algorithm Description

The NWRA AVOSS Prediction Algorithm computes trailing vortex trajectories and circulation decay in a plane perpendicular to the path of the aircraft that has generated the vortices. Underlying the algorithm are the following assumptions:

- initial vortex conditions assume that all trailing vorticity due to lift is rolled up into a vortex pair;
- away from the ground, the vortices are transported laterally at the speed of the local crosswind, and transport due to large-scale turbulence is not included;
- crosswind shear effects are not included, except as might arise from the previous assumption;
- the circulation decay rate for each member of the vortex pair is the same.

For the purpose of the algorithm, the vortices are considered to migrate through four distinct phases. The algorithm treats each of these four phases in a different way, but handles the transitions between phases in a "seamless" manner so that the output of the algorithm makes no distinction between the phases.

Phase I treats the evolution of the vortices away from the ground (see Fig. 1a). Vortex behavior during this phase is described by equations based on those presented by Sarpkaya (2000). Phase II begins when the vortices first start to "feel" the effect of the ground, but are not close enough to the ground to cause the generation of secondary vorticity (see Fig. 1b). Phase III begins when the vortices approach close enough to the ground that their interaction with the ground produces secondary vorticity. Phase IV is an extension of Phase III that corresponds to the continued generation of vorticity at the ground (see Fig. 1c). If the vortices start out close enough to the ground that they immediately should be in Phase II or Phase III, then Phase I is skipped.

Basic assumptions for the four phases are as follows. In Phase I, we assume that the evolution of the vortices is influenced by atmospheric stratification, cross wind and turbulence effects, and can be described by equations based on those presented by Sarpkaya (2000). The atmospheric conditions are represented by vertical profiles of potential temperature, cross wind, and eddy dissipation rate (EDR). (In an earlier version of APA, the Phase I portion of the algorithm used a vertical profile of turbulent kinetic energy [TKE] rather than eddy dissipation rate to represent the ambient atmospheric turbulence.) The algorithm determines the stratification from the potential temperature profile. At altitudes where the gradient of the temperature is not positive, the stratification is assumed to be neutral.

In Phases II, III and IV, we assume that the evolution of the vortices can be represented by the dynamics of point vortices. In Phase II, we assume that the effect of the ground can be represented by image vortices. In Phase III, we assume that the effects of ground generated countersign vorticity can be represented by the introduction of secondary vortices, and in Phase IV, we assume that further ground generated vorticity can be represented by the introduction of additional secondary vortices. Image vortices are also included in Phases III and IV to maintain a zero vertical velocity at the ground. The circulation decay rate obtained by the end of Phase I is assumed to persist throughout Phases II, III and IV.

For Phase I, the algorithm uses numerical software that solves a system of three ordinary differential equations using a constant time step. For Phases II, III and IV, the algorithm uses numerical software that adaptively (variable time step) solves systems of ordinary differential equations that govern the motion of mutually interacting point vortices. Detailed descriptions of the four phases appear below, and the earlier TKE version of Phase I is described in Appendix A.

In the event that the circulation goes to zero in any of the Phases, execution of the algorithm continues in order to provide AVOSS with a time at which the vortices exit the flight corridor through the corridor's lateral boundaries. During this extended portion of the algorithm's execution, the altitude of the primary vortices is kept constant and their circulation is maintained at zero.

3.1 EDR Version of Phase I (Out of Ground Effect)

Based on the results reported by Sarpkaya (2000), the equations solved by the algorithm for the Phase I evolution are:

$$\begin{aligned} \frac{d}{dt}(Vb^2) &= -b^2 C_2 B(z) - \frac{1}{2\pi} \frac{d}{dt}(b\Gamma_Q) \\ \frac{dz}{dt} &= V \\ \frac{dy}{dt} &= U(z) \end{aligned} \quad (1)$$

where $C_2 = 0.4520$ and $B(z) = \int_{z_0}^z N^2(\zeta) d\zeta$. Here, b is the separation distance between the vortices, which is allowed to vary with time according to an expression given below, V is the vertical speed of the descending vortices ($V < 0$), z is altitude (z_0 is initial altitude), y is lateral position, t is time, and $U(z)$ is the vertical profile of lateral wind. Γ_Q , an expression described below, defines the effect of ambient atmospheric turbulence on the vortices' evolution. The circulation, Γ , about each of the vortices is assumed related to V by the equation, $\Gamma = 2\pi bV$. In the above expression for $B(z)$, $N^2(\zeta)$ is the square of the Brunt-Väisälä frequency, and is defined as follows:

$$N^2(\zeta) = \frac{g}{(T + T_0)} \left(\frac{dT}{d\zeta} + \gamma \right), \text{ where } T(\zeta) \text{ is the vertical temperature profile (}^\circ\text{C), } T_0 \text{ is } 273.15$$

$^\circ\text{C}$, g is 9.81 m/sec^2 , and γ , the dry adiabatic lapse rate, is $0.00976 \text{ }^\circ\text{C/m}$.

The Phase I portion of the algorithm solves the above three equations starting from the conditions $V = V_0$, $z = z_0$, and $y = y_0$, the initial values of the vortices vertical speed, altitude, and lateral position, respectively. The value for V_0 is determined from $V_0 = W / (2\pi\rho U b_0^2)$, where W is the weight of the aircraft, ρ is the density of the air, U is the forward speed of the aircraft, and b_0 is taken to be the initial separation of the vortices, defined as $(\pi/4)S$, where S is the wing span of the aircraft. The algorithm uses modified versions of the routines RK4 and RKDUMB from Press et al. (1989) to solve the equations.

In eqn. (1), $\Gamma_Q(z)$ is defined as

$$\Gamma_Q(z) = \Gamma_0 \exp \left[- (C + 0.25N^2(z)) \frac{T}{T^*(\varepsilon^*)} \right],$$

where Γ_0 is the initial circulation of the vortices, and C is a constant determined by the approach described in Robins and Delisi (1999) to be 0.55. The term containing $N^2(z)$ is meant to account for the enhancement of circulation decay by stratification, a small effect in most cases. T is time normalized by b_0/V_0 , and $T^*(\varepsilon^*)$ is the normalized time at which a demise event such as Crow linking (Crow [1970]) is assumed to occur. As indicated, T^* is a function of ε^* , a normalized form of the eddy dissipation rate, ε , defined as $\varepsilon^* = (\varepsilon b_0)^{1/3} / V_0$, where ε , ε^* and T^* are functions of z . $\varepsilon(z)$ is generated by an algorithm developed at North Carolina State University with assistance from Nwra (Han et al. 2000). The dependence of T^* on ε^* is defined by Sarpkaya (2000) as follows:

$$\text{if } \varepsilon^* < 0.001, \quad T^* = 9$$

$$\text{if } 0.001 < \varepsilon^* < 0.0121, \quad T^* = 9.18-180\varepsilon^*$$

$$\text{if } 0.0121 < \varepsilon^* < 0.2535 \quad T^* \text{ is obtained by inverting the relation} \\ \varepsilon^* = (T^*)^{1/4} \exp(-0.7 T^*)$$

$$\text{if } \varepsilon^* > 0.2535, \quad T^* = (0.7475 / \varepsilon^*)^{3/4}$$

This prescription defines T^* to be a decreasing function of ε^* . In other words, stronger turbulence results in more rapid linking.

In eqn. (1), b is a function of time, $b(t)$, and is defined in terms of ε^* and T^* as follows:

for $T < T^*$,

$$\frac{b}{b_0} = \frac{(1 + \alpha\varepsilon^*) (1 - \alpha\varepsilon^* \exp(T / T^*))}{(1 - \alpha\varepsilon^*) (1 + \alpha\varepsilon^* \exp(T / T^*))}$$

and for $T > T^*$,

$$\frac{b}{b_0} = \frac{b(T^*)}{b_0} \left\{ 1 - \frac{2e\alpha\varepsilon^* / K}{1 - (e\alpha\varepsilon^*)^2} \left[1 - \exp\left(-K \frac{T - T^*}{T^*}\right) \right] \right\}$$

where $K = 5/\varepsilon^*$, and the constant α is taken to be 0.5 on the basis of numerous comparisons with observations.

The vortex separation $b(t)$ is a slowly decreasing function of time that is meant to model an increase in descent rate due to the perturbation of the vortices' axes due to Crow instability (Crow [1970]). If we assume that the vortices undergo an anti-symmetric sinusoidal perturbation of peak-to-peak amplitude $2ab_0$, where $a < 0.5$, then the average descent speed of the vortices can be shown to be $V_0 / \sqrt{1 - 4a^2}$, which is greater than V_0 . This effect is modeled by $b(t)$.

It is important to note that the form of the equation for V actually solved by the algorithm is:

$$\frac{dV}{dt} = -C_2 B(z) - 2V \left(\frac{1}{b} \frac{db}{dt} \right) + \frac{b_0}{b} \left[M \frac{V_0^2}{b_0} - V_0 \left(\frac{1}{b} \frac{db}{dt} \right) \right] e^{-MT}$$

$$\text{where } M = \frac{(C + 0.25N^2)}{T^*}.$$

Certain weather conditions such as convection cells and vertical shear of the crosswind are not considered by the preceding formulation. These conditions and normal atmospheric variability, perhaps arising from thermals and large-scale eddies, may lead to uncertainties in predictions of how long it takes for a descending vortex pair to clear the path of following aircraft. Estimates of how large these uncertainties may be are presented in Appendix B.

3.2 Phase II

Phase II of the algorithm begins when the vortices descend below an altitude denoted by ZIMFAC * b_0 . Here ZIMFAC stands for "z image factor," and experience has shown that a good value for ZIMFAC is 1.5. At this point in the vortices' evolution, as they approach the ground, the effect of the ground causes the distance between the vortices to increase. The algorithm models this effect by introducing a pair of vortices beneath the ground that are mirror images of the approaching vortices (Fig. 1b). The result is that the vertical velocity at the ground remains identically zero and the vortices move apart as they come closer to the ground. In Phase II, the three equations based on Sarpkaya's work are replaced by a system of eight equations (see below) that describe the motion of a system of four point vortices. The circulation of the vortices is constrained to decrease at the same rate, denoted by DGMDT (standing for "d G a m m a t"), as that occurring just before the transition to Phase II.

The equations solved during Phase II are based on equations 2.8 and 2.9 given by Donaldson and Bilanin (1975). The Phase II equations may be written as:

$$\begin{aligned}
 \frac{dz_1}{dt} &= \frac{1}{2\pi} \sum_{i=2}^4 \frac{\Gamma_i(t)(y_i - y_1)}{r_{i1}^2} \\
 \frac{dy_1}{dt} &= -\frac{1}{2\pi} \sum_{i=2}^4 \frac{\Gamma_i(t)(z_i - z_1)}{r_{i1}^2} + U(z_1) \\
 \frac{dz_2}{dt} &= \frac{1}{2\pi} \sum_{i=1(i \neq 2)}^4 \frac{\Gamma_i(t)(y_i - y_2)}{r_{i2}^2} \\
 \frac{dy_2}{dt} &= -\frac{1}{2\pi} \sum_{i=1(i \neq 2)}^4 \frac{\Gamma_i(t)(z_i - z_2)}{r_{i2}^2} + U(z_2) \\
 \frac{dz_3}{dt} &= \frac{1}{2\pi} \sum_{i=1(i \neq 3)}^4 \frac{\Gamma_i(t)(y_i - y_3)}{r_{i3}^2} \\
 \frac{dy_3}{dt} &= \frac{dy_1}{dt} \\
 \frac{dz_4}{dt} &= \frac{1}{2\pi} \sum_{i=1}^3 \frac{\Gamma_i(t)(y_i - y_4)}{r_{i4}^2} \\
 \frac{dy_4}{dt} &= \frac{dy_2}{dt}
 \end{aligned} \tag{2}$$

where $r_{ij}^2 = (y_i - y_j)^2 + (z_i - z_j)^2$.

Here, subscripts 1 and 2 denote the primary port and starboard vortices, and 3 and 4 denote their mirror images with respect to the ground. The initial values for z_1 and z_2 are equal to z^* , the vortex altitude at the end of Phase I, and the initial values for z_3 and z_4 are the negatives of z_1 and z_2 . For y_1 and y_2 , the initial values are equal to $y^* - b_0/2$ and $y^* + b_0/2$, respectively, where y^* is the last vortex lateral position from Phase I. The initial values for y_3 and y_4 are the same as for y_1 and y_2 , respectively. The initial values for Γ_1 , Γ_2 , Γ_3 , and Γ_4 are $+\Gamma^*$, $-\Gamma^*$, $-\Gamma^*$, and $+\Gamma^*$, respectively, where $\Gamma^* = 2\pi b_0 V^*$, V^* being the last vertical velocity from Phase I (recall that $V^* < 0$, and thus $\Gamma^* < 0$). As mentioned above, the circulation magnitudes continue decreasing at the same rate as the last rate of decrease in Phase I.

Because the vortex motions are potentially more complicated in Phases II, III and IV than they are for Phase I, we use an adaptive numerical solution scheme to solve the above equations and the governing equations for Phases III and IV (see below). The scheme is implemented in the algorithm by using modified versions of the routines RKQC, RK4 and ODEINT from Press et al. (1989).

3.3 Phase III

Phase III begins when the primary vortices descend below an altitude denoted by $ZGEFAC * b_0$. Here, ZGEFAC stands for "z ground effect factor," and ZGEFAC is typically equal to 0.6. It is assumed in Phase III that the vortices are close enough to the ground that secondary vorticity is generated by the vortices' interaction with the ground. We model this secondary vorticity by introducing two new vortices and their images with respect to the ground. The images continue to ensure that vertical velocity at the ground is zero.

The new vortices are specified by their initial position and intensity relative to the primary vortices. We use the parameters GERFAC (standing for "ground effect radius factor") and GEANG (standing for "ground effect angle") to define the initial position of the secondary vortices, and GAMFAC (standing for "Gamma factor") to define the initial ratio between the secondary and primary circulation. $GERFAC * b_0$ is the initial distance between each pair of secondary and primary vortices and $-GEANG$ is the initial rotation angle, θ , of the secondary vortices about the primary vortices, where $\theta = 0$ is immediately below the primary vortices and θ is positive clockwise for the primary port vortex and positive counterclockwise for the primary starboard vortex. In addition, we define a function of θ , THFACF(θ), to model variation in the secondary vorticity as the secondary vortices rotate around the primary vortices under the influence of the velocity fields of the primary vortices. Values of THFACF(θ) vary between 0.0 and 1.0, which correspond to minimum and maximum influence.

Values of GERFAC, GEANG and GAMFAC used in the algorithm, are 0.4, 45.0 and 0.4, respectively. The function THFACF(θ) is defined by the arrays θ (in degrees): 0.0, 45.0, 225.0, 315.0, 360.0 and THFAC(θ): 0.5, 1.0, 0.0, 0.0, 0.5, where the value of THFAC(θ) for an intermediate value of θ is determined by linear interpolation. For example, $THFAC(112.5^\circ) = 0.625$. The above definition of THFACF(θ) describes secondary vorticity that is strongest at $\theta = 45^\circ$ (90° greater than the initial rotation angle) and weakest after an additional 180° rotation about the main vortex.

In Phase III, there are eight vortices (two primary vortices, each with a secondary vortex, and two image vortices, each with a secondary vortex). Consequently, sixteen equations are required to describe the vortices' evolution for Phase III instead of the eight required for Phase II. The eight new equations are as follows, where subscripts 5 and 6 denote the secondary vortices generated by the port and starboard main vortices (denoted by subscripts 1 and 2), and subscripts 7 and 8 denote their images with respect to the ground:

$$\begin{aligned} \frac{dz_5}{dt} &= \frac{1}{2\pi} \sum_{i=1(i \neq 5)}^8 \frac{\Gamma_i(t)(y_i - y_5)}{r_{i5}^2} \\ \frac{dy_5}{dt} &= -\frac{1}{2\pi} \sum_{i=1(i \neq 5)}^8 \frac{\Gamma_i(t)(z_i - z_5)}{r_{i5}^2} + U(z_5) \\ \frac{dz_6}{dt} &= \frac{1}{2\pi} \sum_{i=1(i \neq 6)}^8 \frac{\Gamma_i(t)(y_i - y_6)}{r_{i6}^2} \end{aligned}$$

$$\begin{aligned}
\frac{dy_6}{dt} &= -\frac{1}{2\pi} \sum_{i=1(i \neq 6)}^8 \frac{\Gamma_i(t)(z_i - z_6)}{r_{i6}^2} + U(z_6) \\
\frac{dz_7}{dt} &= \frac{1}{2\pi} \sum_{i=1(i \neq 7)}^8 \frac{\Gamma_i(t)(y_i - y_7)}{r_{i7}^2} \\
\frac{dy_7}{dt} &= \frac{dy_5}{dt} \\
\frac{dz_8}{dt} &= \frac{1}{2\pi} \sum_{i=1}^7 \frac{\Gamma_i(t)(y_i - y_8)}{r_{i8}^2} \\
\frac{dy_8}{dt} &= \frac{dy_6}{dt} .
\end{aligned} \tag{3}$$

Here it is assumed that initially $\Gamma_i(t) = -\text{GAMFAC} * \text{THFACF}(\text{GEANG}) * \Gamma_{i-4}(t)$ for $i = 5$ and 6 , and $\Gamma_i(t) = -\Gamma_{i-2}(t)$ for $i = 7$ and 8 . Recall that $i = 5, 6, 7$, and 8 denote secondary vortices. As the vortices evolve, the magnitudes of the circulations, Γ_i ($i=5,6,7,8$), are constrained to decrease at a rate proportional to $\text{GAMFAC} * \text{DGMDT}$. In addition, the strengths of the secondary vortices are modulated by $\text{THFACF}(\theta_i)$. The magnitudes of the circulations for $i=1,2,3,4$ continue to decrease at the rate DGMDT . Also note that the previous eight equations (equation set (2)) are the same as before, except that the summations now have an upper limit of 8 (instead of 4), and the last summation also has an upper limit of 8 (instead of 3) with the proviso that the summation excludes $i=4$.

Recently, F. Proctor has proposed a model for circulation decay in ground effect that is based on results from simulations using the TASS Code. The TASS Code and the circulation decay model are described by Proctor (1987), and Proctor et al. (2000), respectively. In Proctor's model, the decay rate increases shortly after the vortices start to interact with the ground (i.e., shortly after the beginning of Phase III in APA), and then relaxes to a nominal level as the vortices move away from the ground. Details of this model are provided in Appendix C.

3.4 Phase IV

Phase IV begins as soon as one of the secondary vortices rotates 180 degrees about the primary vortex with which it is coupled. At this time, two additional ground effect vortices are introduced in the same manner as was done for the Phase III ground effect vortices. The result is two secondary vortices rotating about each primary vortex (Fig. 1c), a configuration that simulates the continuous generation of secondary vorticity due to ground effect. Also, by including all the image vortices (for secondary as well as primary vortices), we assure that vertical velocity at the ground remains identically zero.

There are now twelve vortices; so twenty-four equations are required to represent the evolution for Phase IV. The eight new equations are as follows, where subscripts 9 and 10 denote the new secondary vortices generated by the port and starboard main vortices (denoted by subscripts 1 and 2), and subscripts 11 and 12 denote their images with respect to the ground:

$$\frac{dz_9}{dt} = \frac{1}{2\pi} \sum_{i=1(i \neq 9)}^{12} \frac{\Gamma_i(t)(y_i - y_9)}{r_{i9}^2}$$

$$\begin{aligned}
\frac{dy_9}{dt} &= -\frac{1}{2\pi} \sum_{i=1(i \neq 9)}^{12} \frac{\Gamma_i(t)(z_i - z_9)}{r_{i9}^2} + U(z_9) \\
\frac{dz_{10}}{dt} &= \frac{1}{2\pi} \sum_{i=1(i \neq 10)}^{12} \frac{\Gamma_i(t)(y_i - y_{10})}{r_{i10}^2} \\
\frac{dy_{10}}{dt} &= -\frac{1}{2\pi} \sum_{i=1(i \neq 10)}^{12} \frac{\Gamma_i(t)(z_i - z_{10})}{r_{i10}^2} + U(z_{10}) \\
\frac{dz_{11}}{dt} &= \frac{1}{2\pi} \sum_{i=1(i \neq 11)}^{12} \frac{\Gamma_i(t)(y_i - y_{11})}{r_{i11}^2} \\
\frac{dy_{11}}{dt} &= \frac{dy_9}{dt} \\
\frac{dz_{12}}{dt} &= \frac{1}{2\pi} \sum_{i=1}^{11} \frac{\Gamma_i(t)(y_i - y_{12})}{r_{i12}^2} \\
\frac{dy_{12}}{dt} &= \frac{dy_{10}}{dt} .
\end{aligned} \tag{4}$$

The previous sixteen equations (equations sets (2) and (3)) are the same as before except that the summations now have an upper limit of 12 (instead of 8), and the summation in the equation for dz_8/dt excludes $i = 8$.

If z_0 (the initial altitude) is close enough to the ground that $z_0 \leq \text{ZIMFAC} * b_0$, then only one Phase I time step is computed (to determine DGMDT) and Phase II immediately begins. If z_0 is so close to the ground that $z_0 \leq \text{ZGEFAC} * b_0$ (which should be less than $\text{ZIMFAC} * b_0$), then one Phase I time step is computed to determine DGMDT, Phase II is skipped, and Phase III is begun.

The duration of the evolution computed by the algorithm is bounded by time intervals defined for each of the four phases. These time intervals are necessary to limit the computer memory that is allocated for each phase. Termination of the algorithm will occur if the final time for any of the four phases is reached. However, the time intervals are chosen sufficiently large for the first three phases that the "natural" transition to the next phase will usually occur before the defined final time is reached. Thus, termination of the algorithm should not occur until the Phase IV final time is reached. Current (Version 3.1.1) time intervals for Phases I, II, III and IV, in seconds, are 180, 120, 120 and 120, respectively. Note that the occurrence of an error condition will also terminate the algorithm.

4. Logic Description

A high level description of the algorithm's logic for the case $z_0 > \text{ZIMFAC} * b_0$ is presented below. A flow chart that illustrates this logic appears in Fig. 2.

Main Routine

Obtain aircraft parameters and weather profiles from the Calling Routine.

Define various constants (control parameters) that control the algorithm.

Do **Phase I** and define DGMDT.

If $z < \text{ZIMFAC} * b_0$, Then

Set initial conditions for Phase II.

Do **Phase II**.

If $z < \text{ZGEFAC} * b_0$, Then

Set initial conditions for Phase III.

Do **Phase III**.

If either ground effect vortex rotates 180° , Then

Set initial conditions for Phase IV.

Do **Phase IV**.

Endif

Endif

Endif

Pass primary vortex trajectories and circulations to the Calling Routine.

Phase I

Use modified versions of RK4 and RKDUMB to integrate the three Phase I equations.

Phase II

Use modified versions of RKQC, RK4 and ODEINT to integrate the eight Phase II equations.

Phase III

Use modified versions of RKQC, RK4 and ODEINT to integrate the sixteen Phase III equations.

Phase IV

Use modified versions of RKQC, RK4 and ODEINT to integrate the twenty-four Phase IV equations.

5. Implementation Details

This section contains information that will enable a prospective user of the algorithm to start using it. Subsection 5.1 describes how to invoke the algorithm from a C/C++ calling routine, and subsection 5.2 describes the organization of the algorithm's source code. Included in subsection 5.2 is a discussion of the algorithm's subroutine structure and a description of the contents of the files containing the source code.

5.1 Running the Algorithm

The NWRA AVOSS Prediction Algorithm was originally coded in FORTRAN 77, and was converted to C++ for use within AVOSS. It is structured as a primary function, APA, which provides the link with a calling routine, and makes calls to several supporting functions. The statement that defines APA is as follows:

```
void apa(real yzin, real zzin, real vzin, real bzin,
         int nztdin, const real *tdzin, const real *tdin,
         int nzucin, const real *uczin, const real *ucin,
         int nzqin, const real *qzin, const real *edrin,
         const real *tkein,
         int *ntmout, real *tmout, real *yaout, real *zaout,
         real *gmaout,
         real *ybout, real *zbout, real *gmbout)
```

Here, the declarative "real" is defined in a header file to be equivalent to the C variable type float.

Following are descriptions of the above function arguments, where it is understood that all quantities are given in MKS units. *yzin* and *zzin* are the lateral position and the altitude of the aircraft; *vzin* and *bzin* are the initial descent velocity and separation of the vortices. *nztdin*, *tdzin*, and *tdin* define the temperature profile, where *nztdin* is the number of points in the profile, *tdzin* is an array of altitudes, and *tdin* is an array containing the temperature at each altitude. *nzucin*, *uczin*, and *ucin* define the cross-runway wind profile, where *nzucin* is the number of points in the profile, *uczin* is an array of altitudes, and *ucin* is an array containing the wind speed at each altitude. *nzqin*, *qzin*, *edrin*, and *tkein* define the turbulence profile, where *nzqin* is the number of points in the profile, *qzin* is an array of altitudes, *edrin* is an array containing the eddy dissipation rate at each altitude, and *tkein* is an array containing the turbulence velocity (square root of twice the turbulence kinetic energy) at each altitude. It is assumed that *tdin* contains temperature in degrees Celsius, unless *nztdin* is less than zero, in which case *-nztdin* is the number of points in the temperature profile and *tdin* is assumed to contain potential temperature in degrees Kelvin. For all profiles, data points are expected in order of increasing height, and the crosswind profile must have a point at the ground ($z = 0$).

ntmout is the number of points in the arrays containing the algorithm's predictions. If *ntmout* equals 9999, it means that an error has occurred. It is expected that the calling routine will test for this condition and take appropriate action. *tmout* is an array of times at which the predictions are given. *yaout* and *zaout* are arrays containing predicted lateral positions and altitudes of the port vortex, and *gmaout* is an array containing predicted circulations for the port vortex. *ybout* and *zbout* are arrays containing predicted lateral positions and altitudes of the starboard vortex, and *gmbout* is an array containing predicted circulations for the starboard vortex.

A file called APA.OUT is created each time the algorithm is run. This file contains diagnostic information and can be helpful for determining the cause of errors. Since APA.OUT is overwritten each time the algorithm is called, it is up to the calling routine to save individual versions of APA.OUT if so desired. An outline of what appears in APA.OUT is given in Appendix D, and an example of how multiple versions of APA.OUT can be saved is given in the sample driver program appearing in Appendix E.

The AVOSS Prediction Algorithm may be invoked from the AVOSS software by first declaring and then calling function APA. The declaration statement should be as follows (code fragments appearing below assume that the AVOSS software is written in C/C++):

```

void          extern          apa(float,float,float,float,int,float*,float*,
int,float*,float*,int,float*,float*,float*,
int*,float*,float*,float*,float*,float*,float*,float*);

```

Corresponding to this declaration, the calling statement should be as follows:

```

apa(yz,zz,vz,bz,
nztdeg,tdegz,tdeg,nzucr,ucr,ucr,nzq,qz,edr,tke,
&ntm,tm,ya,za,gama,yb,zb,gamb);

```

Arguments and the function declaration are defined in a header file. A sample driver program containing the above function call is in Appendix E.

Care has been taken in the coding of the prediction algorithm to prevent the occurrence of side effects that could interfere with the AVOSS software. For example, all data passed by reference is immediately copied into temporary arrays to protect data defined in the calling routine. Also, data occupying temporary arrays is constrained not to require more memory than has been allocated.

Appendix F contains test cases, which can be used in conjunction with the implementation and testing of the AVOSS Prediction Algorithm.

5.2 Source Code Organization

The code for the AVOSS Prediction Algorithm is contained in six files: `apa.h`, `apa.c`, `impath2.c`, `gelpth.c`, `ge2pth.c`, and `igsolv.c`. The header file `apa.h` contains definitions of constants, macro functions, structures, and function prototypes. In `apa.c`, the primary function, `APA`, handles the interface with the calling routine, controls the execution of Phase I, and calls the functions, `impath`, `gelpth`, and `ge2pth`, in succession, to execute Phases II, III and IV. These routines are in the files `impath2.c`, `gelpth.c` and `ge2pth.c`, respectively. The file `igsolv.c` contains several routines that are used by the other routines. A complete list of the routines found in each file is given below. A complete listing of the Version 3.1 prediction algorithm code resides with the AVOSS group at NASA's Langley Research Center. Data flow diagrams plus a control flow chart are included in Appendix G.

```

apa.c:
    apa:
    rk dumb:
    derivs:
    rtsafe:
    funcd:
    rk4:
    fk:
impath2.c:
    impath:
    imint:
gelpth.c:
    gelpth:
    gelint:
ge2pth.c:
    ge2pth:
    ge2int:
igsolv.c:
    igdrvs:
    rkqc:
    rk4old:
    gtogl:
    angle:

```

thfacf:

Brief descriptions of each of these routines are as follows:

file `apa.c`:

apa is described above.

rkdumb controls the ordinary differential equation (ODE) solution for Phase I. The solver is based on a routine of the same name from Press et al. (1989) (henceforth called NP, for *Numerical Recipes*).

derivs computes the derivatives required by **rkdumb** and **rk4**.

rtsafe is a nonlinear equation solver based on a routine of the same name from NP.

funcd is a routine that provides values of a given function and its derivatives.

rk4 uses a fourth order Runge-Kutta technique to advance the ODE solution one time step. The technique is based on a routine of the same name in NP.

fk does linear interpolation to obtain values from the environmental profiles.

file `impath2.c`:

impath controls the execution of Phase II.

imint controls the ODE solution for Phase II. The solver is based on the routine ODEINT from NP.

file `ge1pth.c`:

ge1pth controls the execution of Phase III.

ge1int controls the ODE solution for Phase III. The solver is based on the routine ODEINT from NP.

file `ge2pth.c`:

ge2pth controls the execution of Phase IV.

ge2int controls the ODE solution for Phase IV. The solver is based on the routine ODEINT from NP.

file `igsolv.c`:

igdrvs computes the derivatives required by **imint**, **ge1int**, **ge2int**, **rkqc** and **rk4old**.

rkqc controls the step size used in the ODE solutions for Phases II, III and IV. This routine is based on a routine of the same name in NP.

rk4old uses a fourth order Runge-Kutta technique to advance the ODE solution one time step. **rk4old** is a renamed version of **rk4**.

gtogl linearly interpolates the ODE solution onto the output time grid.

angle computes the angle, θ , given by ΔY and ΔX , where $\tan(\theta)$ is given by $\Delta Y / \Delta X$.

thfacf given θ , computes the value of $\text{THFACF}(\theta)$ by linearly interpolating from a table that defines $\text{THFACF}(\theta)$.

Acknowledgements

We gratefully acknowledge the support and encouragement of D. A. Hinton and F. H. Proctor of NASA's Langley Research Center.

References

- Batchelor, G.K. (1970), *An Introduction to Fluid Dynamics*, Cambridge University Press.
- Corjon, A., and T. Poinso (1996), "Vortex Model to Define Safe Aircraft Separation Distances," *Journal of Aircraft*, Vol. 33, No. 3, May-June, pp. 547-553.
- Crow, S.C. (1970), "Stability Theory for a pair of Trailing Vortices," *AIAA Journal*, Vol. 8, No. 12, December, pp. 2172-2179.
- Donaldson, C. duP. and A.J. Bilanin (1975), "Vortex Wakes of Conventional Aircraft," AGARDograph No. 204, May.
- Greene, G.C. (1986), "An Approximate Model of Vortex Decay," *Journal of Aircraft*, Vol. 23, No. 7, July, pp. 566-573.
- Han, J., Shen, S., Arya, S. P., and Lin, Y.-L. (2000), "An Estimation of Turbulent Kinetic Energy and Energy Dissipation Rate Based on Atmospheric Boundary Layer Similarity Theory," NASA CR-2000-210298.
- Hinton, D.A. (1996), "An Aircraft Vortex Spacing System (AVOSS) for Dynamical Vortex Spacing Criteria," Proceedings from the AGARD Fluid Dynamics Panel Symposium held in Trondheim, Norway, 20-23 May, AGARD-CP-584, pp. 23-1 to 23-12.
- Hinton, D.A., J. K. Charnock, and D. R. Bagnell (2000), "Design of an Aircraft Vortex Spacing System for Airport Capacity Improvement," AIAA Paper 2000-0622, 38th Aerospace Sciences Meeting, January 10-13, Reno.
- Liu, H.-T. (1991), "Tow-Tank Simulation of Vortex Wake Dynamics," in Proceedings of the Aircraft Wake Vortices Conference, J.N. Hallock, Ed., FAA Report SD-92, October.
- Press, W.H., B.P. Flannery, S.A. Teukolsky, and W.T. Vetterling (1989), *Numerical Recipes (FORTRAN Version)*, Cambridge University Press.
- Proctor, F.H. (1987), "The Terminal Area Simulation System. Volume I: Theoretical Formulation," NASA Contractor Rep. 4046, NASA, Washington, D.C., April.
- Proctor, F.H., D. W. Hamilton, and J. Han (2000), "Wake Vortex Transport and Decay in Ground Effect: Vortex Linking with the Ground," AIAA Paper 2000-0757, 38th Aerospace Sciences Meeting, January 10-13, Reno.
- Robins, R.E. and D.P. Delisi (1999), "Further Development of a Wake Vortex Prediction Algorithm and Comparisons to Data," AIAA Paper 99-0757, 37th Aerospace Sciences Meeting, January 11-14, Reno.
- Robins, R.E. and D.P. Delisi (2002), "Wake Vortex Algorithm Scoring Results," NASA/CR-2002-211745, June.
- Sarpkaya, T. (2000), "New Model for Vortex Decay in the Atmosphere," *Journal of Aircraft*, Vol. 37, No. 1, January-February, pp. 53-61.

Figures

On the following pages are Figs. 1a – 1c, and Fig. 2. Descriptions of these figures are as follows:

Figure 1. Schematic representation of vortex positions for (a) Phase I, (b) Phase II, and (c) Phase III.

Figure 2. Flowchart for the basic logic of the prediction algorithm.

Out of Ground Effect

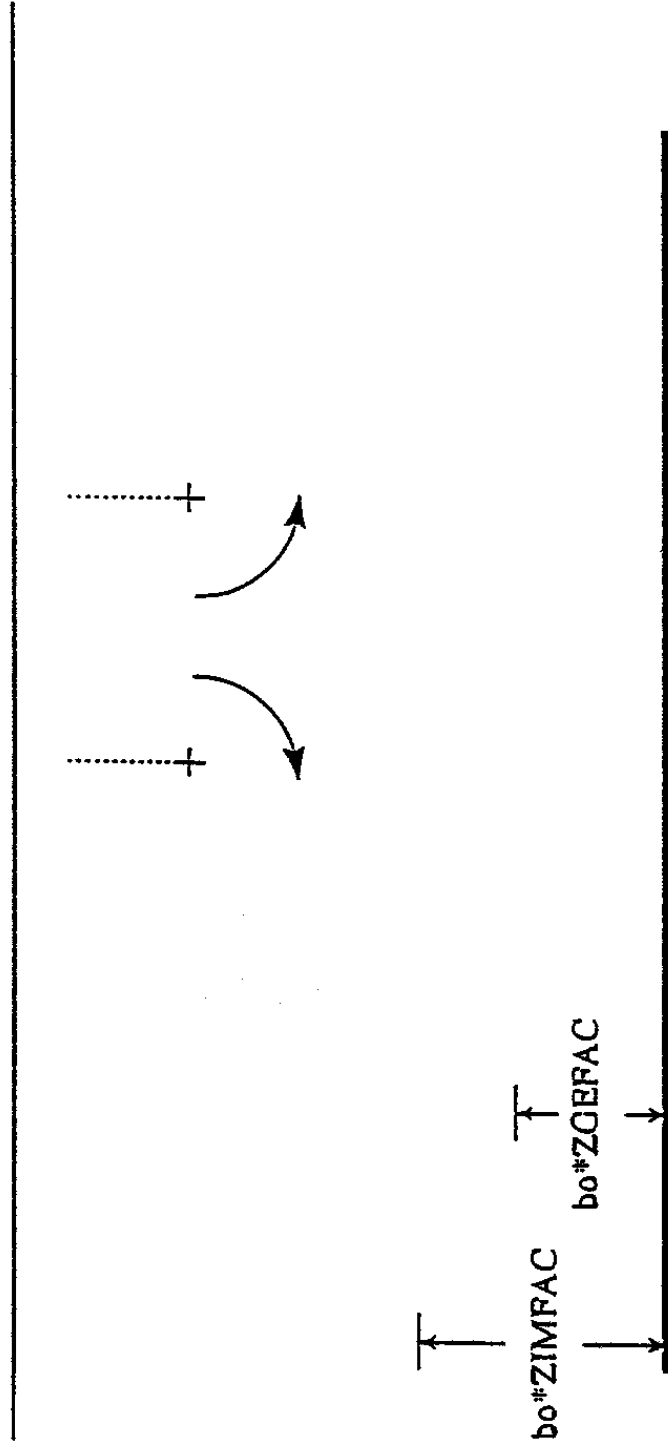


Figure 1a.

Near Ground Effect

0.3

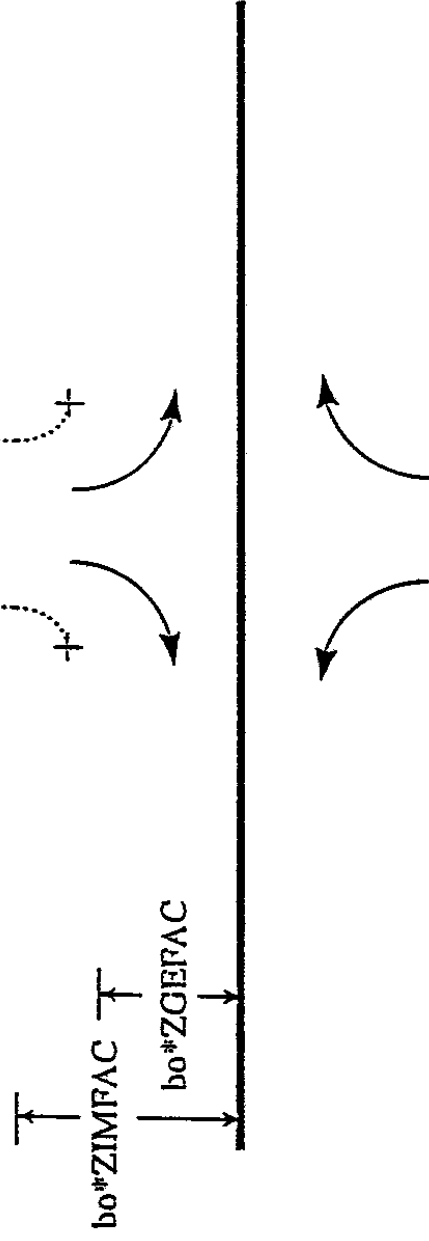


Figure 1b.

In Ground Effect

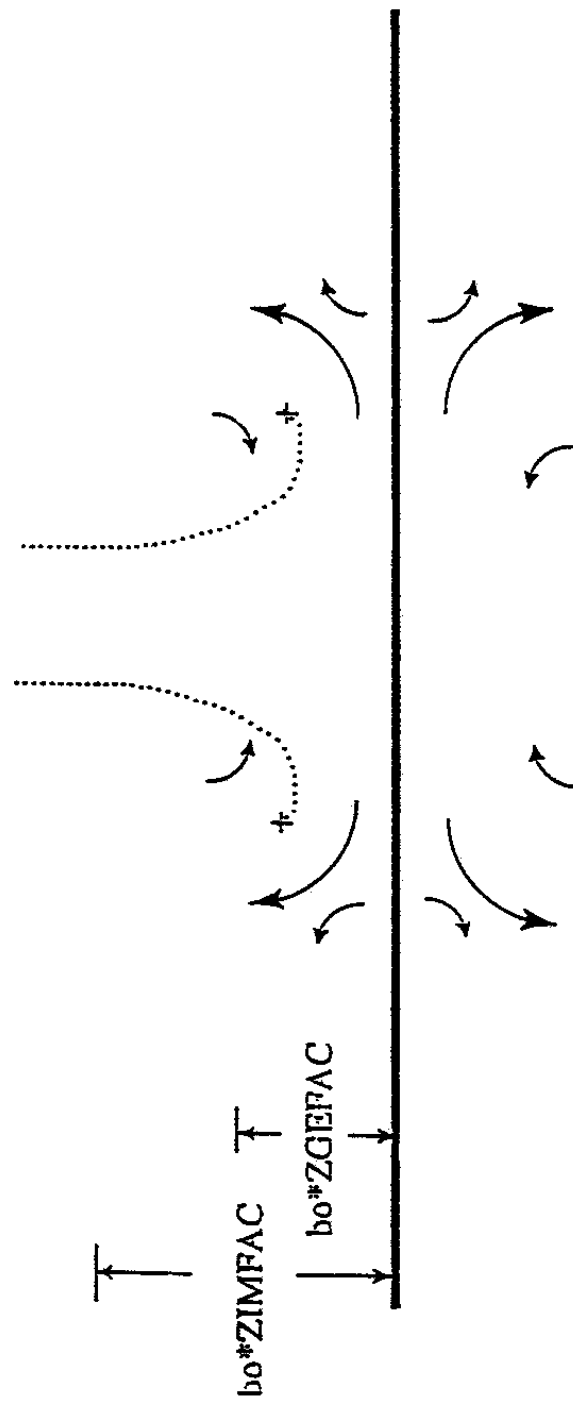


Figure 1c.

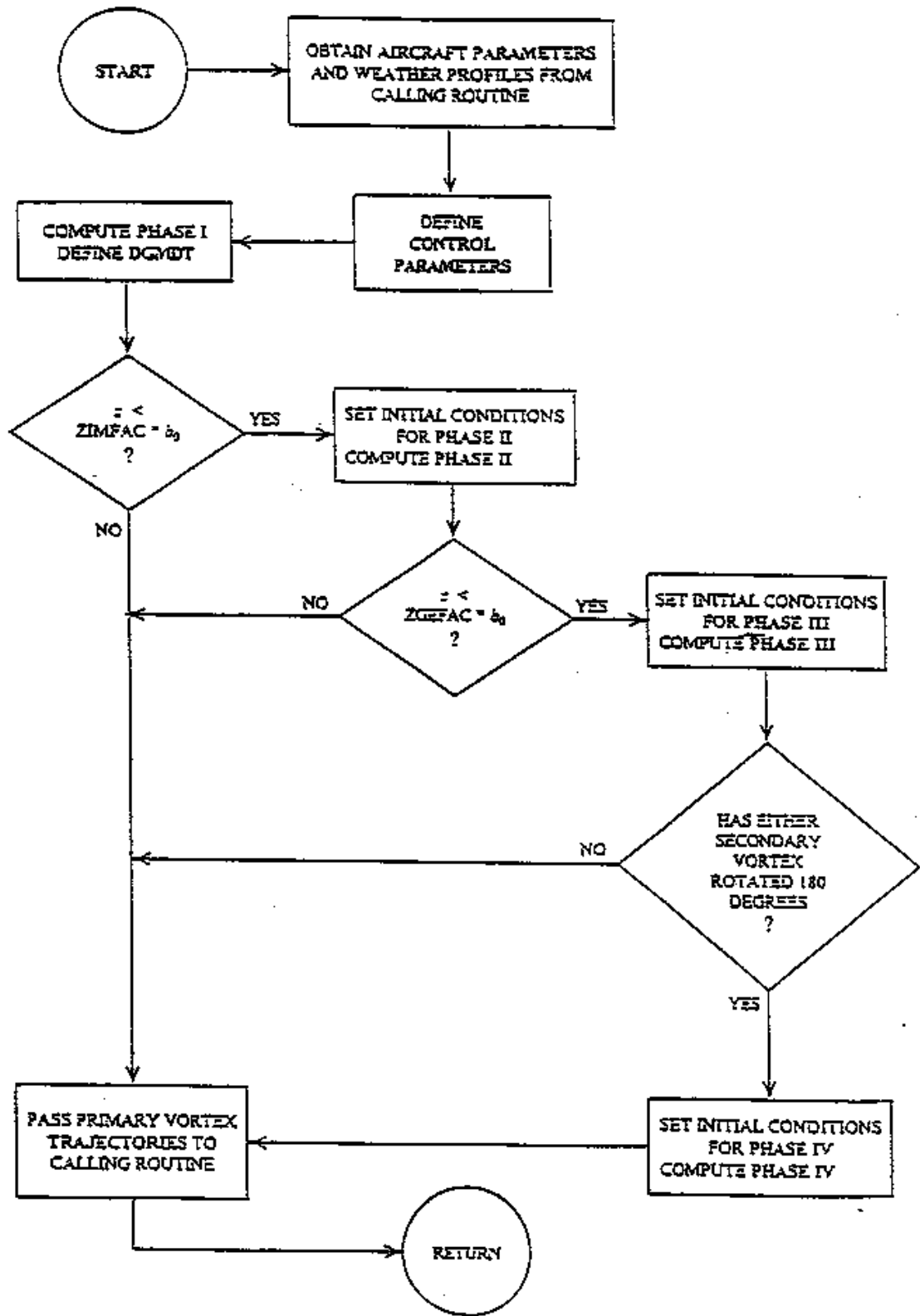


Figure 2.

Appendix A. TKE Version of Phase I.

In an earlier version of APA, the Phase I portion of the algorithm used a vertical profile of turbulent kinetic energy (TKE) rather than eddy dissipation rate (EDR) to represent the ambient atmospheric turbulence. The equations solved in this TKE version of Phase I were based on the work of Greene (1986), and are as follows:

$$\begin{aligned}\frac{dV}{dt} &= -C_1 C_D V^2 (\text{sign}(V)) - C_2 b(z) - C_3 V q(z) \\ \frac{dz}{dt} &= V \\ \frac{dy}{dt} &= U(z)\end{aligned}$$

where $C_1 = 0.1663 / b_0$, $C_2 = 0.4520$, $C_3 = k / b_0$, and $b(z) = \int_{z_0}^z N^2(\zeta) d\zeta$. Here, V is the vertical speed of the descending vortices ($V < 0$), z is altitude (z_0 is initial altitude), y is lateral position, t is time, b_0 is the initial distance between the vortices (vortex separation), and $q(z)$ and $U(z)$ are vertical profiles of root mean square turbulence velocity (square root of twice the turbulence kinetic energy) and lateral wind, respectively. k is a constant, determined by the approach described in Robins and Delisi (1999) to be 0.20. The vertical profile, $q(z)$, is generated using the method of Han et al. (2000). TKE values are typically derived from 30 min. averages of 10 Hz data.

The drag coefficient, C_D , and the square of the Brunt-Väisälä frequency, $N^2(\zeta)$, are defined as follows:

$C_D = 0.2$ for $\text{Re} < 400,000$, $C_D = 1.4$ for $\text{Re} > 600,000$, and C_D varies linearly between 0.2 and 1.4 for $400,000 \leq \text{Re} \leq 600,000$, where Re is defined to be the Reynolds number based on wake oval width and is given by $2.09 b_0 V / \nu$, ν being (temperature dependent) kinematic viscosity. The table of temperature versus kinematic viscosity from Appendix 1 of Batchelor (1970) is used to define ν .

$$N^2(\zeta) = \frac{g}{(T + T_0)} \left(\frac{dT}{dz} + \gamma \right), \text{ where } T(z) \text{ is the vertical temperature profile } (^\circ\text{C}), T_0 \text{ is}$$

273.15 °C, g is 9.81 m/sec², and γ , the dry adiabatic lapse rate, is 0.00976 °C/m.

The circulation, Γ , about each of the vortices is assumed related to V by the theoretical equation, $\Gamma = 2\pi b_0 V$.

The initial conditions for the above three equations are $V = V_0$, $z = z_0$, and $y = y_0$, which represent the vortices' initial vertical speed, altitude, and lateral position, respectively. The initial value V_0 is determined from $V_0 = W / (2\pi\rho U b_0^2)$, where W is the weight of the aircraft, ρ is the density of the air, U is the forward speed of the aircraft, and b_0 is taken to be $(\pi/4)S$, where S is the wing span of the aircraft. Note that $V_0 < 0$, and that each of the three terms on the right hand side of the above first equation are positive. Each term thus contributes to a decrease in the descent rate of the vortices. The equations were solved using modified versions of the routines RK4 and RKDUMB from Press et al. (1989).

Appendix B. Corrections for Time to Leave Corridor

In this appendix, we present several plots of the relationship between atmospheric parameters and the difference between observed and predicted time for vortices to clear the AVOSS corridor. We call this difference the "exceedance" of the observation with respect to the prediction. Note that this definition of exceedance differs from the definition of exceedance used by AVOSS (see Hinton et al. [2000]). Also note that circulation decay is not considered, so it is possible that in some instances of large exceedance, the vortices may have decayed to a sufficiently low level that the exceedance is not operationally significant.

The plots show data from the AVOSS database described by Robins and Delisi (2000). For each plot, we use the results to propose a systematic correction for the predicted time to leave the corridor. The atmospheric parameters shown here were selected from several other atmospheric parameters included in the database because they appeared to have the most potential for leading to a systematic correction that could eventually be included in AVOSS.

On all plots, the exceedance (EXC) is shown on the x-axis and an atmospheric parameter is shown on the y-axis. The first three plots (Figures B-1, B-2 and B-3) show results for vortices in a stable atmosphere and the final two plots (Figures B-4 and B-5) are for an unstable atmosphere, where the sign of the vertical potential temperature gradient (DC/DZ) determines whether or not the atmosphere is stable (positive for stable, negative for unstable). All plots show data from the 1995 Memphis (circles) and the 1997 Dallas/Fort Worth (triangles) deployments.

The atmospheric parameter in Figure B-1 is the reciprocal of the average Froude number (FRAV) over the observed vortex trajectory (by Froude number, we mean V_0 / Nb_0 , where these quantities are defined in Section 3.1). The figure shows that many of the observed clearance times are well predicted, but that exceedances tend to occur for cases with higher stratification (higher $1/\text{FRAV}$). A possible correction to the APA predictions based on this data might be as follows:

```
if (DC/DZ > 0) then
    if (FRAV < 2.5) then add 50
    else if (FRAV < 8) then add 30
    else add 5
endif
endif
```

In other words, if the atmosphere is stable, always add at least 5 seconds to the prediction and add additional time depending on the stratification.

In Figure B-2, the atmospheric parameter is the reciprocal of the Froude number at the vortices' initial altitude ($1/\text{FRZ}$), and the result is similar to that of Figure B-1. Here a possible correction scheme might be as follows:

```
if (DC/DZ > 0) then
    if (FRZ < 3) then add 50
    else if (FRZ < 12) then add 30
    else add 5
endif
endif
```

In Figure B-3, the picture is similar to the previous figures. In this case, the atmospheric parameter is the Brunt-Väisälä frequency at the vortices' initial altitude (NZ), and a possible correction scheme might be as follows:

```
if (DC/DZ > 0) then
    if (NZ > 0.02) then add 50
    else if (NZ > 0.005) then add 30
    else add 5
endif
```

```
endif
endif
```

For the data shown in Figures B-4 and B-5, the atmosphere was unstable ($DC/DZ < 0$), and the atmospheric parameters selected were the eddy dissipation rate from 30 minute chunks of 40m tower data (EDR30) and the normalized eddy dissipation rate averaged over the observed vortex trajectory (EAVN).

For Figure B-4, a correction scheme might be:

```
if (DC/DZ < 0) then
  if (EDR30 > 0.001) then add 30
  else add 10
endif
endif
```

And for Figure B-5, a correction scheme might be:

```
if (DC/DZ < 0) then
  if (EAVN > 0.18) then add 30
  else add 10
endif
endif
```

In other words, if the atmosphere is unstable, always add at least 10 seconds to the prediction and add additional time depending on the eddy dissipation rate.

Note that all of the above schemes should be viewed as preliminary, and further evaluation of observations and predictions under various atmospheric conditions will be required before such schemes can be included in production versions of AVOSS.

DC / DZ > 0

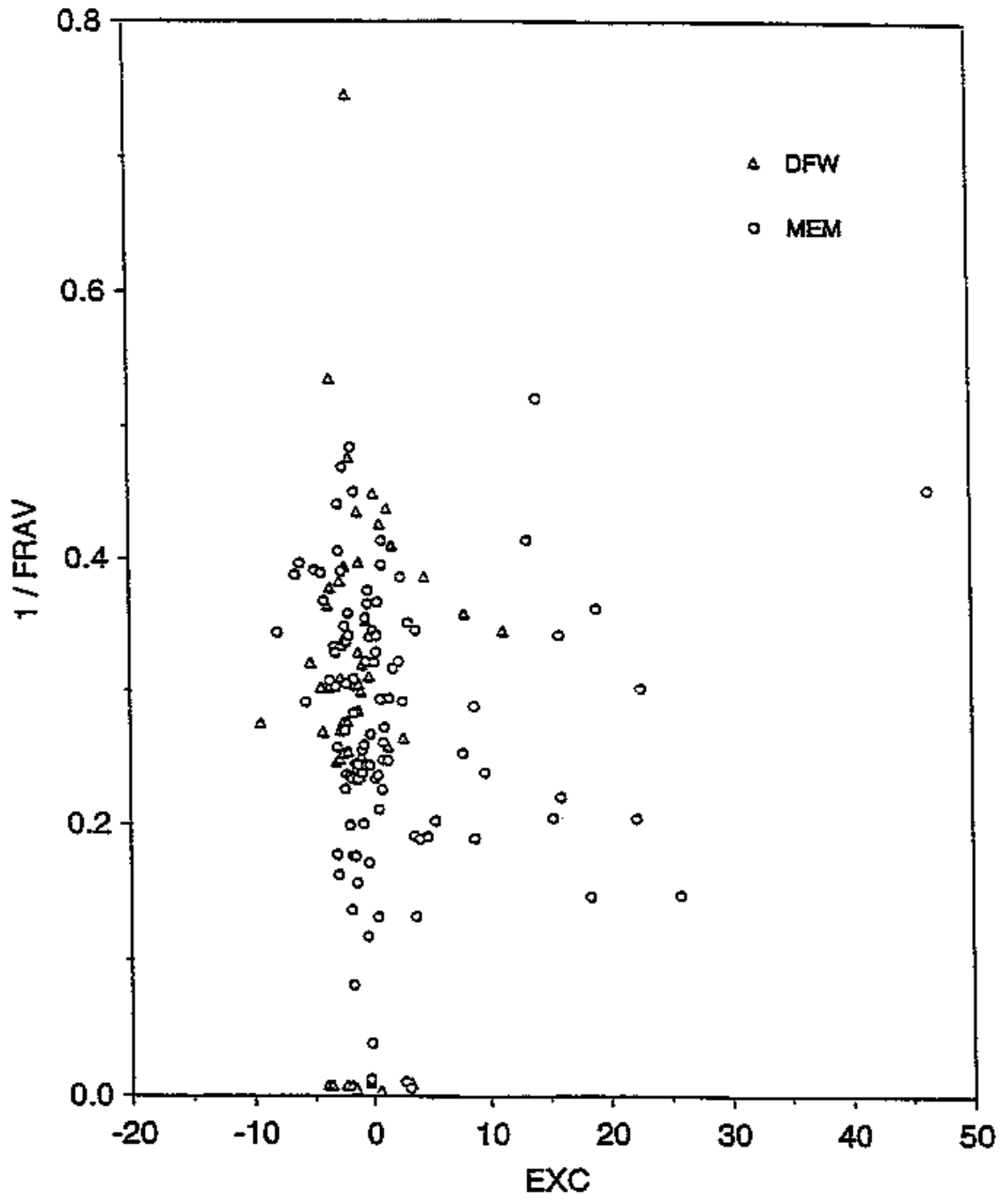


Figure B-1

DC / DZ > 0

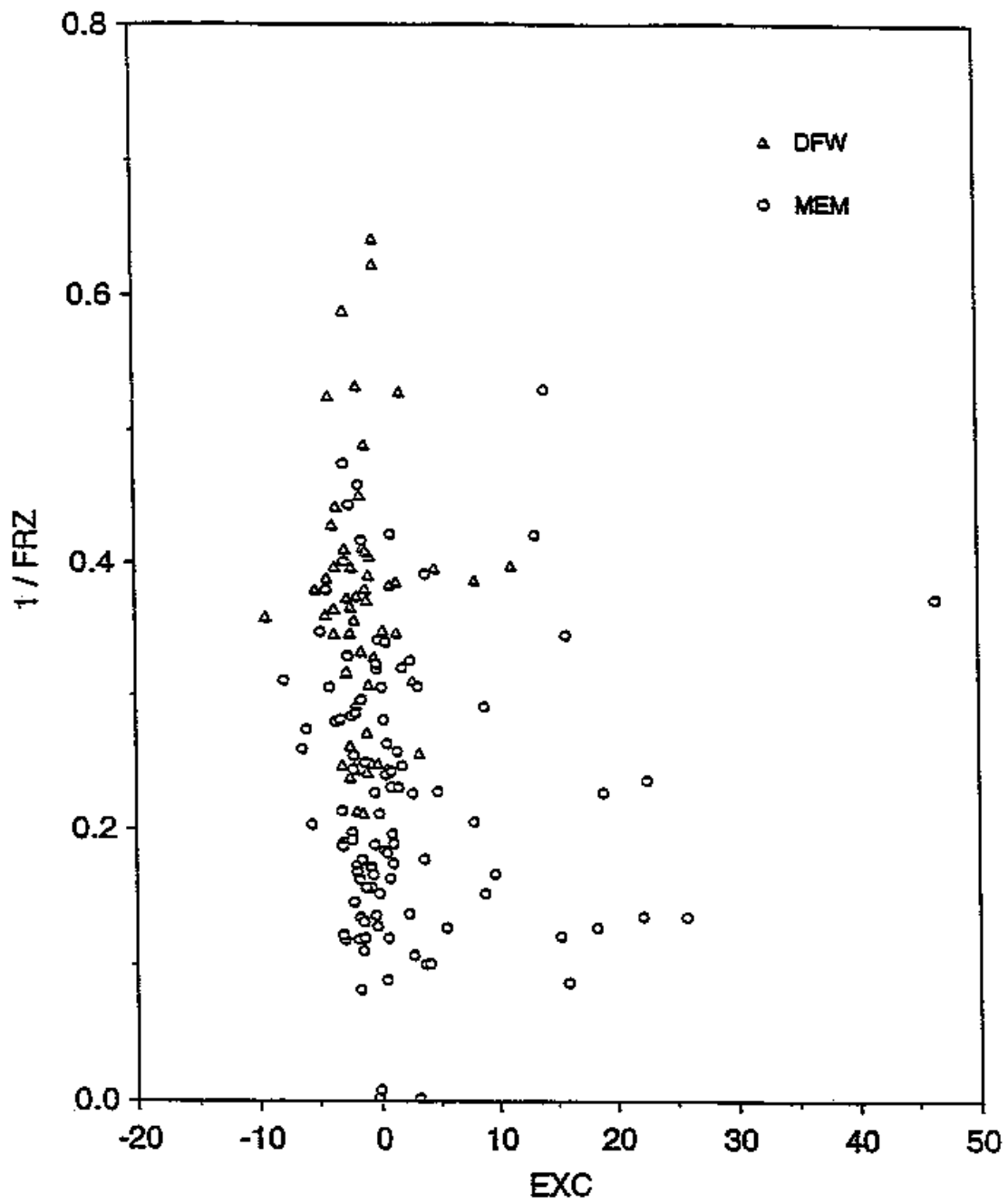


Figure B-2

DC / DZ > 0

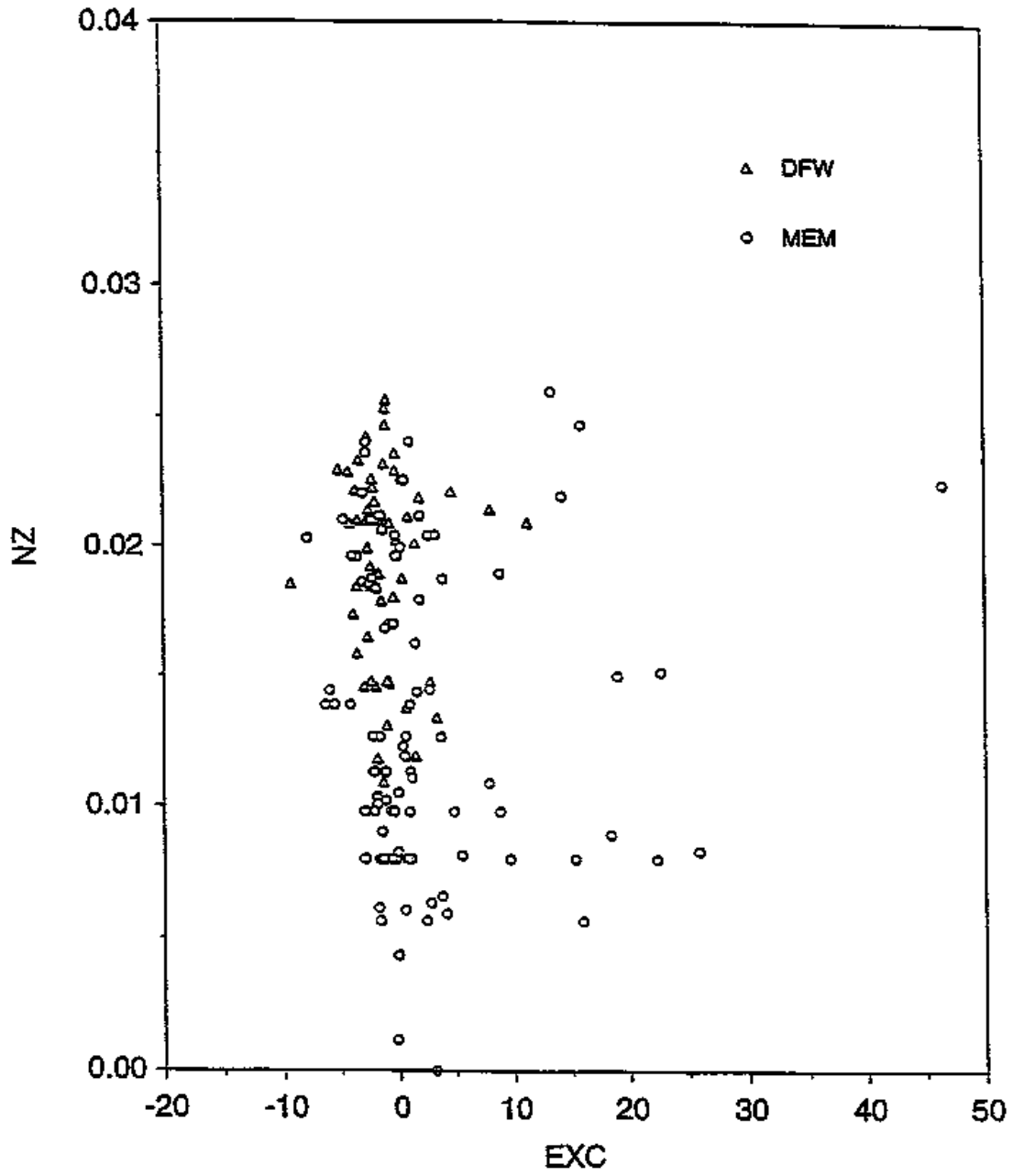


Figure B-3

DC / DZ < 0

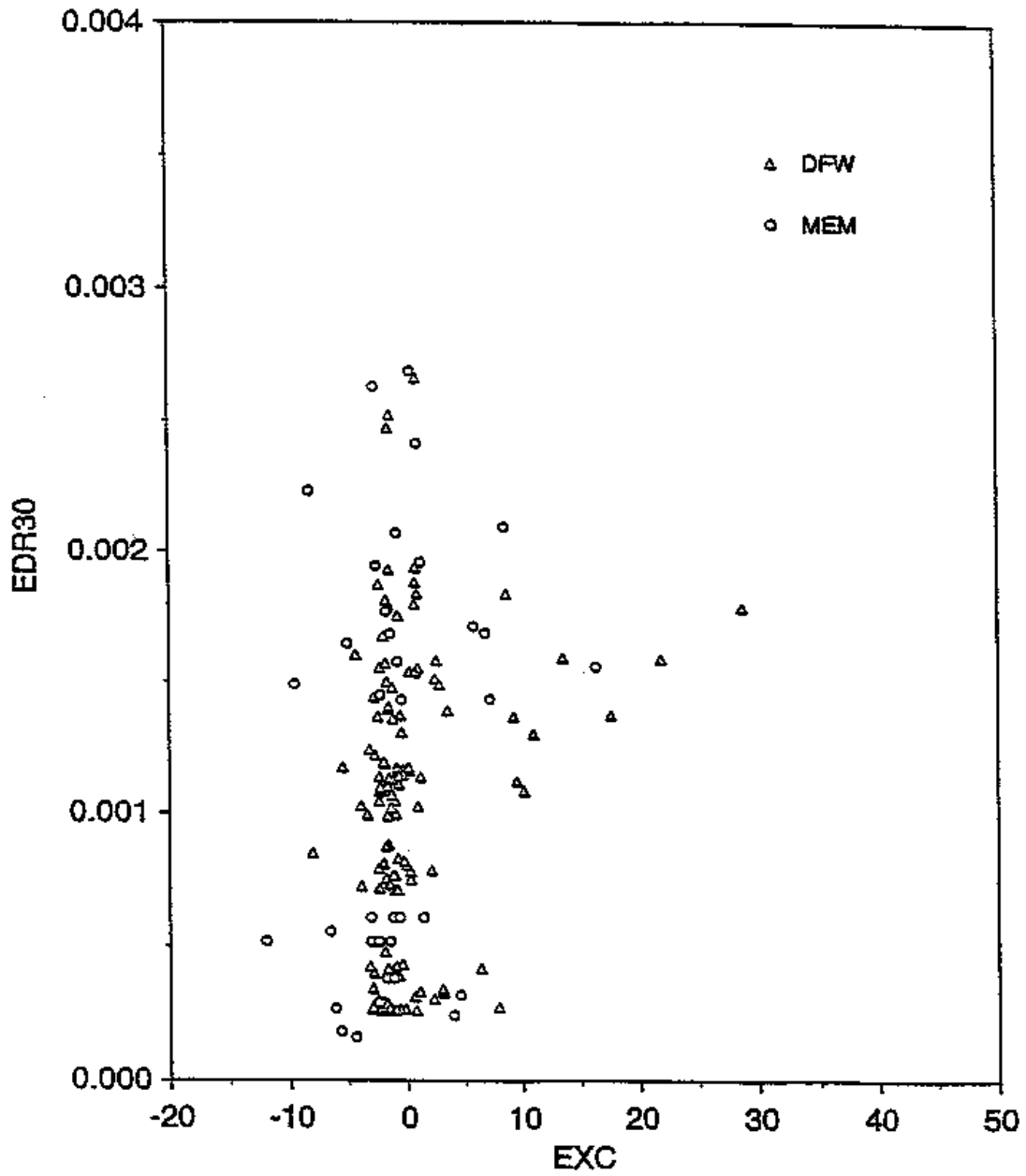


Figure B-4

DC / DZ < 0

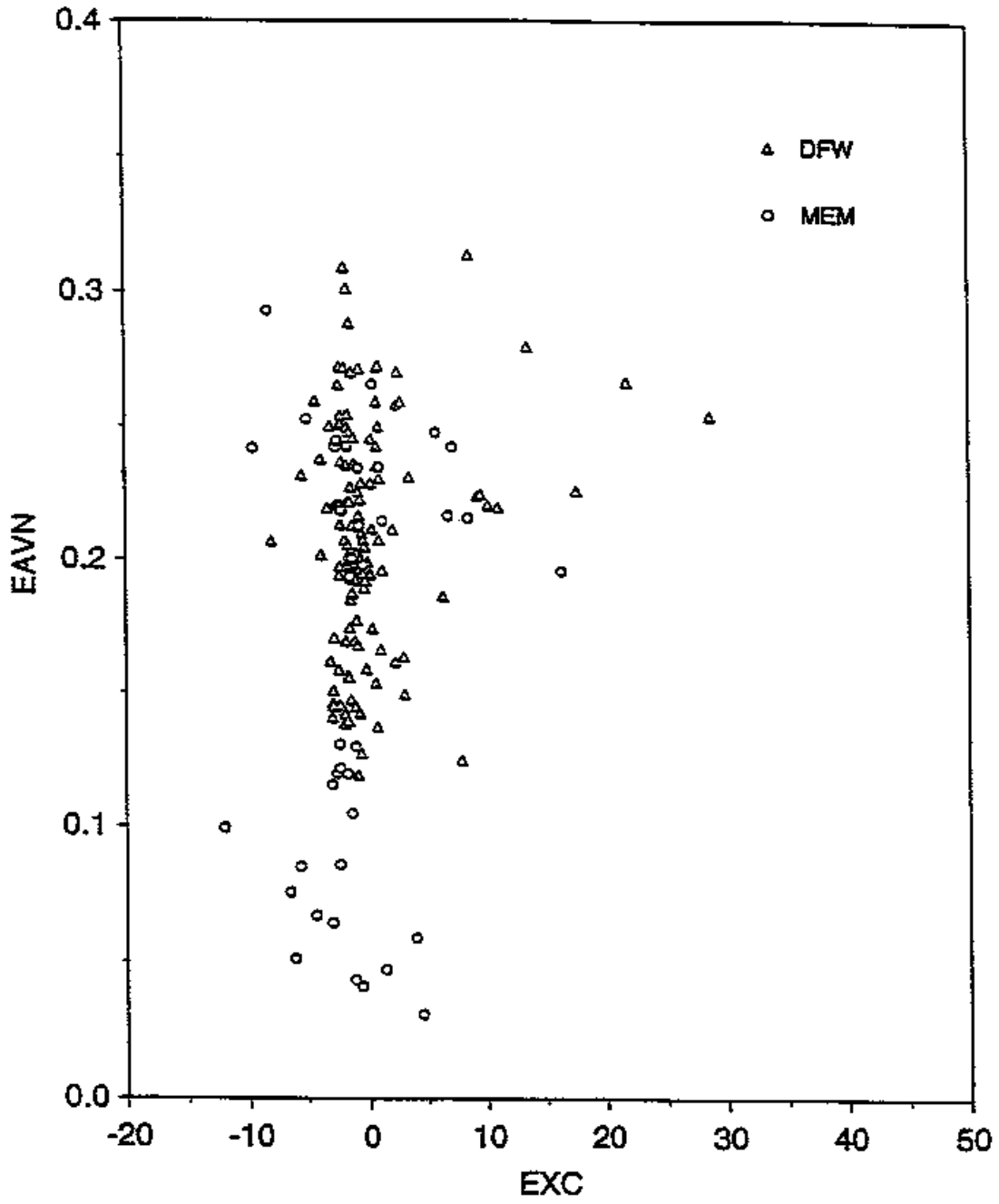


Figure B-5

Appendix C. Circulation Decay Model for Ground Interaction

In this appendix, we describe a model proposed by Proctor et al. (2000) for the circulation decay of vortices interacting with the ground. Recall, that the current prediction algorithm assumes that the rate of circulation decay is fixed for Phases II, III, and IV, at a constant rate equal to the rate that occurs at the end of Phase I, just before the transition to Phase II. Let us express this rate as the non-dimensional constant, $D_0 = (1/\Gamma_0)d\Gamma/dT$, where Γ is circulation, Γ_0 is initial circulation, and T is time normalized by b_0 / V_0 .

Then, according to Proctor's analysis of results from TASS simulations of vortices in ground effect, once the vortices reach their minimum altitude at a non-dimensional time T_G , the vortices' circulation decay may be expressed as

$$D(T) = d\Gamma^* / dT = -(4/15)(T - T_{GG})^{-1/3} \exp[-0.4(T - T_{GG})^{2/3}]$$

where $\Gamma^* = \Gamma / \Gamma_0$, and $T_{GG} = T_G + 0.25$.

We have implemented this model in the current algorithm, for testing purposes, by applying the above expression for $T > T_G + 0.4$, and computing $D(T)$ for $T_G < T < T_G + 0.4$ by linearly interpolating between D_0 and $D(T_G + 0.4)$. As T increases, the above expression for $D(T)$ eventually increases exponentially, so the second part of the model is to constrain $d\Gamma^* / dT$ to not exceed -0.125, a nominal value of non-dimensional circulation decay observed in previous deployments.

Evaluation of Proctor's model by comparison with observations of vortices in ground effect is currently underway. When the AVOSS prediction algorithm eventually includes this model, the algorithm version number will be 3.2.

Appendix D. Description of APA.OUT

Note that for purposes of emphasis and clarity, variables appearing in the following appendices do not always have the same case as they have in the listings.

Appearing below is a sample of the diagnostic output file APA.OUT. It starts off with the primary control parameters (**yz** through **Hmin**) that were used for the run that produced the file. These are followed by a table (GAMMA ROTATION DECAY) defining the function THFACF(θ) (see Section 3.3). Next appears three tables defining the temperature, crosswind, and turbulence profiles used by the algorithm. Finally APA.OUT contains a table showing how the separation between the vortices and the circulation vary with time, followed by the circulation decay rate (INITIAL DGMDT) at the end of Phase I, which is also used throughout Phases II, III and IV. This is followed by the circulation decay rates for the four vortices used in Phase II, the magnitudes of which are equal to "INITIAL DGMDT." Following all this are the parameters **vz** through **yover**, which are described as follows:

vz is repeated from earlier in the table, **z_{im}** is the altitude below which Phase II begins, **z_{ge}** is the altitude below which Phase III begins, **gerad** is the distance between the secondary, ground effect vortices and the primary vortices, **gamfac** is the ratio of the circulation of the secondary vortices to the circulation of the primary vortices, and **zdown** and **yover** give the vertical and horizontal affects of the secondary vortices from the primary vortices.

Items appearing in APA.OUT not yet described are:

t1,t2,Nt through **T1_ge2,T2_ge2,Nt_ge2** define the time intervals and output time resolution for Phases I, II, III and IV. Starting and ending times and the number of time points are given for each phase.

kmax, Dtfac, Eps, H1 and **Hmin** are parameters that control the numerical software adapted from Press et al. (1989).

Except for **yz, zz, vz, bz**, and the environmental profiles, the items listed in APA.OUT are preset by the algorithm and not user provided.

SAMPLE OF APA.OUT

```
yz = 0.000000e+00    zz = 2.500000e+01    vz = 1.723000e+00    bz = 2.984500e+01
zimfac = 1.500000e+00  zgefacc = 6.000000e-01  gamfac = 4.000000e-01
gerfac = 4.000000e-01  geang = 4.500000e+01
```

```
t1 = 0.000000e+00    t2 = 1.800000e+02    Nt = 181
t1_img = 0.000000e+00    t2_img = 1.200000e+02    Nt_img = 121
T1_ge1 = 0.000000e+00    T2_ge1 = 1.200000e+02    Nt_ge1 = 121
T1_ge2 = 0.000000e+00    T2_ge2 = 1.200000e+02    Nt_ge2 = 121
```

```
kmax = 4000    Dtfac = 1.000000e-02    Eps = 1.000000e-06
H1 = 1.000000e-02
Hmin = 1.000000e-10
```

GAMMA ROTATION DECAY

ANGLE	FACTOR
0.00000	0.50000
15.00000	0.66667
30.00000	0.83333
45.00000	1.00000

60.00000	0.91667
75.00001	0.83333
90.00000	0.75000
105.00001	0.66667
120.00000	0.58333
135.00000	0.50000
150.00001	0.41667
165.00001	0.33333
180.00001	0.25000
195.00000	0.16667
210.00001	0.08333
225.00000	0.00000
240.00001	0.00000
255.00000	0.00000
270.00000	0.00000
285.00000	0.00000
300.00002	0.00000
315.00002	0.00000
330.00002	0.16667
344.99999	0.33333
360.00001	0.50000

 Index Height Temperature

0	0.50000	24.11000
1	1.65000	23.87000
2	3.05000	23.76000
3	4.74000	23.67000
4	6.78000	23.60000
5	9.25000	23.54000
6	12.24000	23.47000
7	15.85000	23.41000
8	20.22000	23.35000
9	25.51000	23.28000
10	31.90000	23.20000
11	39.63000	23.11000
12	48.98000	23.02000
13	60.29000	22.90000
14	73.97000	22.93000
15	90.51000	23.20000
16	110.52000	23.60000
17	134.71001	24.24000
18	163.97000	25.33000
19	199.36000	25.12000
20	242.17000	25.07000
21	293.94000	25.50000
22	353.94000	26.28000
23	413.94000	26.51000
24	473.94000	26.28000
25	533.94000	25.71000
26	593.94000	25.15000
27	653.94000	24.64000
28	713.94000	24.42000
29	773.94000	23.92000
30	833.94000	23.42000
31	893.94000	23.25000

32	953.94000	22.78000
33	1013.94000	22.26000
34	1073.93994	21.97000
35	1133.93994	21.55000
36	1193.93994	21.09000
37	1253.93994	20.56000
38	1313.93994	20.12000
39	1373.93994	19.57000

Index	Height	Cross-Wind
-------	--------	------------

0	0.00000	-2.26000
1	5.00000	-3.70000
2	10.00000	-3.84000
3	15.00000	-4.17000
4	30.00000	-4.25000
5	45.00000	-4.26000
6	60.00000	-4.33000
7	100.00000	-4.27000
8	150.00000	-4.31000
9	200.00000	-4.26000
10	250.00000	-4.48000
11	300.00000	-4.80000
12	350.00000	-5.44000
13	400.00000	-5.88000
14	450.00000	-5.71000
15	500.00000	-5.52000
16	550.00000	-5.78000
17	600.00000	-5.97000

Index	Height	EDR	TKE
-------	--------	-----	-----

0	0.00000	0.00020	0.10000
1	1000.00000	0.00020	0.10000

***** Separation History *****

t,sep,gam =
0.000000 29.844999 -323.099854
1.000000 29.795235 -320.309265

Initial DGMDT = 2.79059
DGAM = 2.79059 -2.79059 -2.79059 2.79059

vz = 1.723000e+00 zim = 2.475000e+01 zge = 1.787714e+01
gerad = 1.191809e+01 gamfac = 4.000000e-01 zdown = 8.427365e+00
yover = 8.427365e+00

Appendix E. Sample Algorithm Driver

Appearing below is a listing of a sample driver for the prediction algorithm. Written in C, and thus compatible with C++, this driver is intended to be a guide for how the algorithm can be utilized from C or C++. The section of code starting with `/* SAMPLE ACTION FOLLOWS */` is an example of how multiple versions of the diagnostic output file APA.OUT can be saved in a cumulative diagnostic output file called DIAG.OUT. The algorithm's trajectory and circulation decay prediction for the port and starboard vortices are written by the driver to the file TRAJEC.DAT. The constants NZMAX and NTMMAX, and the declaration for function `apa` are contained in the header file APA.H.

```
*****
Sample of Algorithm Driver
*****
#include "apa.h"
#include <stdio.h>
#include <stdlib.h>
#include <time.h>

FILE *fp_tdeg, *fp_ucr, *fp_q, *fp_trajec;
FILE *fp_diag;

time_t now;

main()
{
    float yz,zz,vz,bz;

    int i,nztdeg,nzucr,nzq;
    float tdegz[NZMAX],tdeg[NZMAX];
    float ucrz[NZMAX],ucr[NZMAX];
    float qz[NZMAX],edr[NZMAX],tke[NZMAX]

    int ntm,rsig;
    float tm[NTMMAX],ya[NTMMAX],za[NTMMAX],gama[NTMMAX],
        yb[NTMMAX],zb[NTMMAX],gamb[NTMMAX];

/* DEFINE AIRPLANE DATA */

    yz = 0.; /* AIRCRAFT CROSS-RUNWAY POSITION (M) */
    zz = 150.; /* AIRCRAFT ALTITUDE (M) */
    vz = 1.723; /* INITIAL VORTEX DESCENT RATE (M/SEC) */
    bz = 29.845; /* INITIAL VORTEX SEPARATION (M) */

/* DEFINE TEMPERATURE DATA (DEG C) */

    fp_tdeg = fopen("TDATA","r");
    fscanf(fp_tdeg,"%d\n",&nztdeg);
    for(i=0; i<nztdeg; i++)
        fscanf(fp_tdeg,"%f %f\n", tdegz + i, tdeg + i);
    fclose(fp_tdeg);

/* DEFINE CROSS-WIND DATA */

    fp_ucr = fopen("UDATA","r");
    fscanf(fp_ucr,"%d\n",&nzucr);
```

```

for(i=0; i<nzucr; i++)
    fscanf(fp_ucr,"%f %f\n", ucrz + i, ucr + i);
fclose(fp_ucr);

/* DEFINE TURBULENCE DATA */

fp_q = fopen("QDATA","r");
fscanf(fp_q,"%d\n",&nzq);
for(i=0; i<nzq; i++)
    fscanf(fp_q,"%f %f\n", qz + i, edr + I,tketi);
fclose(fp_q);

/* INITIALIZE TRAJECTORY DATA */

ntm = 0;
for(i=0; i<NTMMAX; i++) {
    tm[i] = 0.;
    gama[i] = ya[i] = za[i] = 0.;
    gamb[i] = yb[i] = zb[i] = 0.;
}

/* CALL ALGORITHM */

apa(yz,zz,vz,bz,                /* AIRCRAFT DATA */
    nztdeg,tdegz,tdeg,          /* TEMPERATURE DATA */
    nzucr,ucr,z,ucr,            /* CROSS-WIND DATA */
    nzq,qz,edr,tke,             /* TURBULENCE DATA */
    &ntm,tm,ya,za,gama,yb,zb,gamb); /* TRAJECTORY DATA */

/* NOTE: ntm == 9999 indicates a bad run;
    check the file APA.OUT for diagnostic output */

/* TAKE ACTION IF ntm == 9999 */

/* SAMPLE ACTION FOLLOWS */
rsig = 0;
if(ntm == 9999) {
    fp_diag = fopen("DIAG.OUT","a");
    fprintf(fp_diag,"\n*****\n");
    now = time(NULL);
    fprintf(fp_diag,"%s",ctime(&now));
    fclose(fp_diag);
    printf("***** ERROR RETURN FROM APA *****\n");
    system("cat APA.OUT >> DIAG.OUT");
    ntm = NTMMAX;
    rsig = -1;
}

/* PROCESS VORTEX CIRCULATION AND TRAJECTORY PREDICTIONS */

fp_trajec = fopen("TRAJEC.DAT","w");
fprintf(fp_trajec," TIME LY LZ LCIRC RY RZ RCIRC\n");
for(i=0; i<ntm; i++)
    fprintf(fp_trajec,"%8.3f,%9.3f,%9.3f,%9.3f,%9.3f,%9.3f,%9.3f\n",
        tm[i],ya[i],za[i],gama[i],yb[i],zb[i],gamb[i]);
fclose(fp_trajec);

```

```
    return(rsig);  
}
```

Appendix F. Test Cases

Appearing on the following pages are the APA.OUT and TRAJEC.DAT files (see Appendices D and E) produced for three test cases. For all cases, the aircraft is a B-757, and the temperature and crosswind profiles are based on data taken during NASA's September 1997 Dallas deployment. These profiles are presented in the APA.OUT files. The initial aircraft altitudes for Cases 1, 2 and 3 are 150, 50 and 25 meters, respectively. For all cases the eddy dissipation rate is set to a constant $0.002 \text{ m}^2/\text{sec}^3$.

In the TRAJEC.DAT files, the headings TIME, LY, LZ, LCIRC, RY, RZ, and RCIRC refer to the time in seconds, the lateral position, altitudes and circulation for the port vortex, and the lateral position, altitude and circulation for the starboard vortex. All units are MKS.

APA.OUT for TEST CASE # 1

yz = 0.000000e+00 zz = 1.500000e+02 vz = 1.723000e+00 bz = 2.984500e+01
zimfac = 1.500000e+00 zgefacs = 6.000000e-01 gamfac = 4.000000e-01 gerfac = 4.000000e-01
geang = 4.500000e+01
t1 = 0.000000e+00 t2 = 1.800000e+02 Nt = 181
t1_img = 0.000000e+00 t2_img = 1.200000e+02 Nt_img = 121
T1_ge1 = 0.000000e+00 T2_ge1 = 1.200000e+02 Nt_ge1 = 121
T1_ge2 = 0.000000e+00 T2_ge2 = 1.200000e+02 Nt_ge2 = 121
kmax = 4000 Dtfac = 1.000000e-02 Eps = 1.000000e-06 H1 = 1.000000e-02
Hmin = 1.000000e-10

GAMMA ROTATION DECAY

ANGLE	FACTOR
0.00000	0.50000
15.00000	0.66667
30.00000	0.83333
45.00000	1.00000
60.00000	0.91667
75.00001	0.83333
90.00000	0.75000
105.00001	0.66667
120.00000	0.58333
135.00000	0.50000
150.00001	0.41667
165.00001	0.33333
180.00001	0.25000
195.00000	0.16667
210.00001	0.08333
225.00000	0.00000
240.00001	0.00000
255.00000	0.00000
270.00000	0.00000
285.00000	0.00000
300.00002	0.00000
315.00002	0.00000
330.00002	0.16667
344.99999	0.33333
360.00001	0.50000

Index	Height	Temperature
0	0.50000	24.11000
1	1.65000	23.87000
2	3.05000	23.76000
3	4.74000	23.67000
4	6.78000	23.60000
5	9.25000	23.54000
6	12.24000	23.47000
7	15.85000	23.41000
8	20.22000	23.35000
9	25.51000	23.28000
10	31.90000	23.20000
11	39.63000	23.11000
12	48.98000	23.02000
13	60.29000	22.90000
14	73.97000	22.93000

15	90.51000	23.20000
16	110.52000	23.60000
17	134.71001	24.24000
18	163.97000	25.33000
19	199.36000	25.12000
20	242.17000	25.07000
21	293.94000	25.50000
22	353.94000	26.28000
23	413.94000	26.51000
24	473.94000	26.28000
25	533.94000	25.71000
26	593.94000	25.15000
27	653.94000	24.64000
28	713.94000	24.42000
29	773.94000	23.92000
30	833.94000	23.42000
31	893.94000	23.25000
32	953.94000	22.78000
33	1013.94000	22.26000
34	1073.93994	21.97000
35	1133.93994	21.55000
36	1193.93994	21.09000
37	1253.93994	20.56000
38	1313.93994	20.12000
39	1373.93994	19.57000

Index	Height	Cross-Wind
0	0.00000	-2.26000
1	5.00000	-3.70000
2	10.00000	-3.84000
3	15.00000	-4.17000
4	30.00000	-4.25000
5	45.00000	-4.26000
6	60.00000	-4.33000
7	100.00000	-4.27000
8	150.00000	-4.31000
9	200.00000	-4.26000
10	250.00000	-4.48000
11	300.00000	-4.80000
12	350.00000	-5.44000
13	400.00000	-5.88000
14	450.00000	-5.71000
15	500.00000	-5.52000
16	550.00000	-5.78000
17	600.00000	-5.97000

Index	Height	EDR	TKE
0	0.00000	0.00020	0.10000
1	1000.00000	0.00020	0.10000

***** Separation History *****

t,sep,gam =		
0.000000	29.844999	-323.099854
1.000000	29.795235	-319.608276
2.000000	29.744768	-315.928009
3.000000	29.693586	-312.061157
4.000000	29.641678	-308.009979

5.000000	29.589039	-303.776978
6.000000	29.535658	-299.364655
7.000000	29.481525	-294.775665
8.000000	29.426634	-290.012817
9.000000	29.370970	-285.078979
10.000000	29.314531	-280.091675
11.000000	29.257305	-275.000488
12.000000	29.199278	-269.789490
13.000000	29.140448	-264.461151
14.000000	29.080799	-259.017944
15.000000	29.020325	-253.462326
16.000000	28.959013	-247.796936
17.000000	28.896860	-242.024460
18.000000	28.833849	-236.147568
19.000000	28.769976	-230.169006
20.000000	28.705223	-224.091553
21.000000	28.639587	-217.918106
22.000000	28.573059	-211.651535
23.000000	28.505625	-205.294754
24.000000	28.437273	-198.850754
25.000000	28.367998	-192.322556
26.000000	28.297785	-185.713196
27.000000	28.226629	-179.025787
28.000000	28.154512	-172.263412
29.000000	28.081436	-165.470840
30.000000	28.007374	-158.631134
31.000000	27.932333	-151.740250
32.000000	27.856291	-144.800644
33.000000	27.779240	-137.814880
34.000000	27.701168	-130.785553
35.000000	27.622068	-123.715202
36.000000	27.541935	-116.606445
37.000000	27.460739	-109.461777
38.000000	27.378490	-102.283852
39.000000	27.295168	-95.075241
40.000000	27.210764	-87.838509
41.000000	27.125265	-80.576241
42.000000	27.038662	-73.291008
43.000000	26.950949	-65.985405
44.000000	26.862103	-58.661953
45.000000	26.772127	-51.323246
46.000000	26.681002	-43.971809
47.000000	26.588722	-36.610188
48.000000	26.495274	-29.240885
49.000000	26.400648	-21.866413
50.000000	26.304829	-14.489249
51.000000	26.207817	-7.111869
52.000000	26.109591	0.000000
53.000000	26.010145	0.000000
54.000000	25.909470	0.000000
55.000000	25.807554	0.000000
56.000000	25.704390	0.000000
57.000000	25.599957	0.000000
58.000000	25.494253	0.000000
59.000000	25.387272	0.000000
60.000000	25.278994	0.000000
61.000000	25.169415	0.000000
62.000000	25.058523	0.000000
63.000000	24.946312	0.000000
64.000000	24.834988	0.000000
65.000000	24.767487	0.000000
66.000000	24.735434	0.000000

67.000000	24.720215	0.000000
68.000000	24.712990	0.000000
69.000000	24.709557	0.000000
70.000000	24.707926	0.000000
71.000000	24.707153	0.000000
72.000000	24.706785	0.000000
73.000000	24.706612	0.000000
74.000000	24.706530	0.000000
75.000000	24.706490	0.000000
76.000000	24.706470	0.000000
77.000000	24.706461	0.000000
78.000000	24.706457	0.000000
79.000000	24.706455	0.000000
80.000000	24.706453	0.000000
81.000000	24.706453	0.000000
82.000000	24.706453	0.000000
83.000000	24.706453	0.000000
84.000000	24.706453	0.000000
85.000000	24.706453	0.000000
86.000000	24.706453	0.000000
87.000000	24.706453	0.000000
88.000000	24.706453	0.000000
89.000000	24.706453	0.000000
90.000000	24.706453	0.000000
91.000000	24.706453	0.000000
92.000000	24.706453	0.000000
93.000000	24.706453	0.000000
94.000000	24.706453	0.000000
95.000000	24.706453	0.000000
96.000000	24.706453	0.000000
97.000000	24.706453	0.000000
98.000000	24.706453	0.000000
99.000000	24.706453	0.000000
100.000000	24.706453	0.000000
101.000000	24.706453	0.000000
102.000000	24.706453	0.000000
103.000000	24.706453	0.000000
104.000000	24.706453	0.000000
105.000000	24.706453	0.000000
106.000000	24.706453	0.000000
107.000000	24.706453	0.000000
108.000000	24.706453	0.000000
109.000000	24.706453	0.000000
110.000000	24.706453	0.000000
111.000000	24.706453	0.000000
112.000000	24.706453	0.000000
113.000000	24.706453	0.000000
114.000000	24.706453	0.000000
115.000000	24.706453	0.000000
116.000000	24.706453	0.000000
117.000000	24.706453	0.000000
118.000000	24.706453	0.000000
119.000000	24.706453	0.000000
120.000000	24.706453	0.000000
121.000000	24.706453	0.000000
122.000000	24.706453	0.000000
123.000000	24.706453	0.000000
124.000000	24.706453	0.000000
125.000000	24.706453	0.000000
126.000000	24.706453	0.000000
127.000000	24.706453	0.000000
128.000000	24.706453	0.000000

129.000000	24.706453	0.000000
130.000000	24.706453	0.000000
131.000000	24.706453	0.000000
132.000000	24.706453	0.000000
133.000000	24.706453	0.000000
134.000000	24.706453	0.000000
135.000000	24.706453	0.000000
136.000000	24.706453	0.000000
137.000000	24.706453	0.000000
138.000000	24.706453	0.000000
139.000000	24.706453	0.000000
140.000000	24.706453	0.000000
141.000000	24.706453	0.000000
142.000000	24.706453	0.000000
143.000000	24.706453	0.000000
144.000000	24.706453	0.000000
145.000000	24.706453	0.000000
146.000000	24.706453	0.000000
147.000000	24.706453	0.000000
148.000000	24.706453	0.000000
149.000000	24.706453	0.000000
150.000000	24.706453	0.000000
151.000000	24.706453	0.000000
152.000000	24.706453	0.000000
153.000000	24.706453	0.000000
154.000000	24.706453	0.000000
155.000000	24.706453	0.000000
156.000000	24.706453	0.000000
157.000000	24.706453	0.000000
158.000000	24.706453	0.000000
159.000000	24.706453	0.000000
160.000000	24.706453	0.000000
161.000000	24.706453	0.000000
162.000000	24.706453	0.000000
163.000000	24.706453	0.000000
164.000000	24.706453	0.000000
165.000000	24.706453	0.000000
166.000000	24.706453	0.000000
167.000000	24.706453	0.000000
168.000000	24.706453	0.000000
169.000000	24.706453	0.000000
170.000000	24.706453	0.000000
171.000000	24.706453	0.000000
172.000000	24.706453	0.000000
173.000000	24.706453	0.000000
174.000000	24.706453	0.000000
175.000000	24.706453	0.000000
176.000000	24.706453	0.000000
177.000000	24.706453	0.000000
178.000000	24.706453	0.000000
179.000000	24.706453	0.000000

TRAJEC.DAT for TEST CASE #1

TIME	LY	LZ	LCIRC	RY	RZ	RCIRC
0.000,	-14.922,	150.000,	-323.100,	14.922,	150.000,	323.100
1.000,	-19.207,	148.285,	-319.608,	10.588,	148.285,	319.608
2.000,	-23.490,	146.586,	-315.928,	6.255,	146.586,	315.928
3.000,	-27.771,	144.904,	-312.061,	1.923,	144.904,	312.061
4.000,	-32.050,	143.241,	-308.010,	-2.408,	143.241,	308.010
5.000,	-36.328,	141.597,	-303.777,	-6.739,	141.597,	303.777
6.000,	-40.604,	139.973,	-299.365,	-11.068,	139.973,	299.365
7.000,	-44.878,	138.371,	-294.776,	-15.396,	138.371,	294.776
8.000,	-49.150,	136.791,	-290.013,	-19.724,	136.791,	290.013
9.000,	-53.421,	135.234,	-285.079,	-24.050,	135.234,	285.079
10.000,	-57.691,	133.701,	-280.092,	-28.376,	133.701,	280.092
11.000,	-61.958,	132.193,	-275.000,	-32.701,	132.193,	275.000
12.000,	-66.225,	130.710,	-269.789,	-37.025,	130.710,	269.789
13.000,	-70.489,	129.252,	-264.461,	-41.349,	129.252,	264.461
14.000,	-74.752,	127.821,	-259.018,	-45.671,	127.821,	259.018
15.000,	-79.014,	126.417,	-253.462,	-49.993,	126.417,	253.462
16.000,	-83.274,	125.041,	-247.797,	-54.315,	125.041,	247.797
17.000,	-87.532,	123.694,	-242.024,	-58.635,	123.694,	242.024
18.000,	-91.789,	122.375,	-236.148,	-62.955,	122.375,	236.148
19.000,	-96.044,	121.087,	-230.169,	-67.274,	121.087,	230.169
20.000,	-100.298,	119.829,	-224.092,	-71.593,	119.829,	224.092
21.000,	-104.551,	118.602,	-217.918,	-75.911,	118.602,	217.918
22.000,	-108.802,	117.407,	-211.652,	-80.229,	117.407,	211.652
23.000,	-113.052,	116.244,	-205.295,	-84.546,	116.244,	205.295
24.000,	-117.300,	115.115,	-198.851,	-88.863,	115.115,	198.851
25.000,	-121.547,	114.019,	-192.323,	-93.179,	114.019,	192.323
26.000,	-125.793,	112.957,	-185.713,	-97.495,	112.957,	185.713
27.000,	-130.037,	111.930,	-179.026,	-101.811,	111.930,	179.026
28.000,	-134.280,	110.938,	-172.263,	-106.126,	110.938,	172.263
29.000,	-138.522,	109.982,	-165.471,	-110.441,	109.982,	165.471
30.000,	-142.763,	109.063,	-158.631,	-114.755,	109.063,	158.631
31.000,	-147.002,	108.180,	-151.740,	-119.070,	108.180,	151.740
32.000,	-151.240,	107.334,	-144.801,	-123.384,	107.334,	144.801
33.000,	-155.477,	106.525,	-137.815,	-127.698,	106.525,	137.815
34.000,	-159.713,	105.755,	-130.786,	-132.012,	105.755,	130.786
35.000,	-163.948,	105.023,	-123.715,	-136.326,	105.023,	123.715
36.000,	-168.182,	104.329,	-116.606,	-140.640,	104.329,	116.606
37.000,	-172.414,	103.675,	-109.462,	-144.953,	103.675,	109.462
38.000,	-176.646,	103.060,	-102.284,	-149.267,	103.060,	102.284
39.000,	-180.876,	102.486,	-95.075,	-153.581,	102.486,	95.075
40.000,	-185.106,	101.952,	-87.839,	-157.895,	101.952,	87.839
41.000,	-189.334,	101.458,	-80.576,	-162.209,	101.458,	80.576
42.000,	-193.562,	101.006,	-73.291,	-166.523,	101.006,	73.291
43.000,	-197.789,	100.596,	-65.985,	-170.838,	100.596,	65.985
44.000,	-202.015,	100.227,	-58.662,	-175.153,	100.227,	58.662
45.000,	-206.240,	99.901,	-51.323,	-179.468,	99.901,	51.323
46.000,	-210.465,	99.617,	-43.972,	-183.784,	99.617,	43.972
47.000,	-214.689,	99.376,	-36.610,	-188.101,	99.376,	36.610
48.000,	-218.914,	99.179,	-29.241,	-192.418,	99.179,	29.241
49.000,	-223.138,	99.025,	-21.866,	-196.737,	99.025,	21.866
50.000,	-227.361,	98.915,	-14.489,	-201.057,	98.915,	14.489
51.000,	-231.585,	98.850,	-7.112,	-205.377,	98.850,	7.112
52.000,	-235.807,	98.829,	0.000,	-209.698,	98.829,	-0.000
53.000,	-240.029,	98.829,	0.000,	-214.019,	98.829,	-0.000
54.000,	-244.251,	98.829,	0.000,	-218.341,	98.829,	-0.000
55.000,	-248.471,	98.829,	0.000,	-222.664,	98.829,	-0.000

56.000,	-252.692,	98.829,	0.000,	-226.987,	98.829,	-0.000
57.000,	-256.911,	98.829,	0.000,	-231.311,	98.829,	-0.000
58.000,	-261.130,	98.829,	0.000,	-235.636,	98.829,	-0.000
59.000,	-265.348,	98.829,	0.000,	-239.961,	98.829,	-0.000
60.000,	-269.566,	98.829,	0.000,	-244.287,	98.829,	-0.000
61.000,	-273.783,	98.829,	0.000,	-248.613,	98.829,	-0.000
62.000,	-277.999,	98.829,	0.000,	-252.941,	98.829,	-0.000
63.000,	-282.215,	98.829,	0.000,	-257.268,	98.829,	-0.000
64.000,	-286.431,	98.829,	0.000,	-261.596,	98.829,	-0.000
65.000,	-290.669,	98.829,	0.000,	-265.901,	98.829,	-0.000
66.000,	-294.925,	98.829,	0.000,	-270.189,	98.829,	-0.000
67.000,	-299.189,	98.829,	0.000,	-274.469,	98.829,	-0.000
68.000,	-303.457,	98.829,	0.000,	-278.744,	98.829,	-0.000
69.000,	-307.727,	98.829,	0.000,	-283.017,	98.829,	-0.000
70.000,	-311.998,	98.829,	0.000,	-287.290,	98.829,	-0.000
71.000,	-316.269,	98.829,	0.000,	-291.562,	98.829,	-0.000
72.000,	-320.541,	98.829,	0.000,	-295.834,	98.829,	-0.000
73.000,	-324.813,	98.829,	0.000,	-300.106,	98.829,	-0.000
74.000,	-329.084,	98.829,	0.000,	-304.378,	98.829,	-0.000
75.000,	-333.356,	98.829,	0.000,	-308.650,	98.829,	-0.000
76.000,	-337.628,	98.829,	0.000,	-312.921,	98.829,	-0.000
77.000,	-341.900,	98.829,	0.000,	-317.193,	98.829,	-0.000
78.000,	-346.171,	98.829,	0.000,	-321.465,	98.829,	-0.000
79.000,	-350.443,	98.829,	0.000,	-325.737,	98.829,	-0.000
80.000,	-354.715,	98.829,	0.000,	-330.008,	98.829,	-0.000
81.000,	-358.987,	98.829,	0.000,	-334.280,	98.829,	-0.000
82.000,	-363.258,	98.829,	0.000,	-338.552,	98.829,	-0.000
83.000,	-367.530,	98.829,	0.000,	-342.824,	98.829,	-0.000
84.000,	-371.802,	98.829,	0.000,	-347.095,	98.829,	-0.000
85.000,	-376.074,	98.829,	0.000,	-351.367,	98.829,	-0.000
86.000,	-380.345,	98.829,	0.000,	-355.639,	98.829,	-0.000
87.000,	-384.617,	98.829,	0.000,	-359.911,	98.829,	-0.000
88.000,	-388.889,	98.829,	0.000,	-364.182,	98.829,	-0.000
89.000,	-393.161,	98.829,	0.000,	-368.454,	98.829,	-0.000
90.000,	-397.432,	98.829,	0.000,	-372.726,	98.829,	-0.000
91.000,	-401.704,	98.829,	0.000,	-376.998,	98.829,	-0.000
92.000,	-405.976,	98.829,	0.000,	-381.269,	98.829,	-0.000
93.000,	-410.248,	98.829,	0.000,	-385.541,	98.829,	-0.000
94.000,	-414.519,	98.829,	0.000,	-389.813,	98.829,	-0.000
95.000,	-418.791,	98.829,	0.000,	-394.085,	98.829,	-0.000
96.000,	-423.063,	98.829,	0.000,	-398.356,	98.829,	-0.000
97.000,	-427.335,	98.829,	0.000,	-402.628,	98.829,	-0.000
98.000,	-431.606,	98.829,	0.000,	-406.900,	98.829,	-0.000
99.000,	-435.878,	98.829,	0.000,	-411.172,	98.829,	-0.000
100.000,	-440.150,	98.829,	0.000,	-415.443,	98.829,	-0.000
101.000,	-444.422,	98.829,	0.000,	-419.715,	98.829,	-0.000
102.000,	-448.693,	98.829,	0.000,	-423.987,	98.829,	-0.000
103.000,	-452.965,	98.829,	0.000,	-428.259,	98.829,	-0.000
104.000,	-457.237,	98.829,	0.000,	-432.531,	98.829,	-0.000
105.000,	-461.509,	98.829,	0.000,	-436.802,	98.829,	-0.000
106.000,	-465.781,	98.829,	0.000,	-441.074,	98.829,	-0.000
107.000,	-470.052,	98.829,	0.000,	-445.346,	98.829,	-0.000
108.000,	-474.324,	98.829,	0.000,	-449.618,	98.829,	-0.000
109.000,	-478.596,	98.829,	0.000,	-453.889,	98.829,	-0.000
110.000,	-482.868,	98.829,	0.000,	-458.161,	98.829,	-0.000
111.000,	-487.139,	98.829,	0.000,	-462.433,	98.829,	-0.000
112.000,	-491.411,	98.829,	0.000,	-466.705,	98.829,	-0.000
113.000,	-495.683,	98.829,	0.000,	-470.976,	98.829,	-0.000
114.000,	-499.955,	98.829,	0.000,	-475.248,	98.829,	-0.000
115.000,	-504.226,	98.829,	0.000,	-479.520,	98.829,	-0.000
116.000,	-508.498,	98.829,	0.000,	-483.792,	98.829,	-0.000
117.000,	-512.770,	98.829,	0.000,	-488.063,	98.829,	-0.000
118.000,	-517.042,	98.829,	0.000,	-492.335,	98.829,	-0.000

119.000,	-521.313,	98.829,	0.000,	-496.607,	98.829,	-0.000
120.000,	-525.585,	98.829,	0.000,	-500.879,	98.829,	-0.000
121.000,	-529.857,	98.829,	0.000,	-505.150,	98.829,	-0.000
122.000,	-534.129,	98.829,	0.000,	-509.422,	98.829,	-0.000
123.000,	-538.400,	98.829,	0.000,	-513.694,	98.829,	-0.000
124.000,	-542.672,	98.829,	0.000,	-517.966,	98.829,	-0.000
125.000,	-546.944,	98.829,	0.000,	-522.237,	98.829,	-0.000
126.000,	-551.215,	98.829,	0.000,	-526.509,	98.829,	-0.000
127.000,	-555.487,	98.829,	0.000,	-530.781,	98.829,	-0.000
128.000,	-559.759,	98.829,	0.000,	-535.052,	98.829,	-0.000
129.000,	-564.031,	98.829,	0.000,	-539.324,	98.829,	-0.000
130.000,	-568.302,	98.829,	0.000,	-543.596,	98.829,	-0.000
131.000,	-572.574,	98.829,	0.000,	-547.868,	98.829,	-0.000
132.000,	-576.846,	98.829,	0.000,	-552.139,	98.829,	-0.000
133.000,	-581.118,	98.829,	0.000,	-556.411,	98.829,	-0.000
134.000,	-585.389,	98.829,	0.000,	-560.683,	98.829,	-0.000
135.000,	-589.661,	98.829,	0.000,	-564.955,	98.829,	-0.000
136.000,	-593.933,	98.829,	0.000,	-569.226,	98.829,	-0.000
137.000,	-598.204,	98.829,	0.000,	-573.498,	98.829,	-0.000
138.000,	-602.476,	98.829,	0.000,	-577.770,	98.829,	-0.000
139.000,	-606.748,	98.829,	0.000,	-582.042,	98.829,	-0.000
140.000,	-611.020,	98.829,	0.000,	-586.313,	98.829,	-0.000
141.000,	-615.291,	98.829,	0.000,	-590.585,	98.829,	-0.000
142.000,	-619.563,	98.829,	0.000,	-594.857,	98.829,	-0.000
143.000,	-623.835,	98.829,	0.000,	-599.128,	98.829,	-0.000
144.000,	-628.107,	98.829,	0.000,	-603.400,	98.829,	-0.000
145.000,	-632.378,	98.829,	0.000,	-607.672,	98.829,	-0.000
146.000,	-636.650,	98.829,	0.000,	-611.944,	98.829,	-0.000
147.000,	-640.922,	98.829,	0.000,	-616.215,	98.829,	-0.000
148.000,	-645.193,	98.829,	0.000,	-620.487,	98.829,	-0.000
149.000,	-649.465,	98.829,	0.000,	-624.759,	98.829,	-0.000
150.000,	-653.737,	98.829,	0.000,	-629.031,	98.829,	-0.000
151.000,	-658.009,	98.829,	0.000,	-633.302,	98.829,	-0.000
152.000,	-662.280,	98.829,	0.000,	-637.574,	98.829,	-0.000
153.000,	-666.552,	98.829,	0.000,	-641.846,	98.829,	-0.000
154.000,	-670.824,	98.829,	0.000,	-646.117,	98.829,	-0.000
155.000,	-675.096,	98.829,	0.000,	-650.389,	98.829,	-0.000
156.000,	-679.367,	98.829,	0.000,	-654.661,	98.829,	-0.000
157.000,	-683.639,	98.829,	0.000,	-658.933,	98.829,	-0.000
158.000,	-687.911,	98.829,	0.000,	-663.204,	98.829,	-0.000
159.000,	-692.182,	98.829,	0.000,	-667.476,	98.829,	-0.000
160.000,	-696.454,	98.829,	0.000,	-671.748,	98.829,	-0.000
161.000,	-700.726,	98.829,	0.000,	-676.020,	98.829,	-0.000
162.000,	-704.998,	98.829,	0.000,	-680.291,	98.829,	-0.000
163.000,	-709.269,	98.829,	0.000,	-684.563,	98.829,	-0.000
164.000,	-713.541,	98.829,	0.000,	-688.835,	98.829,	-0.000
165.000,	-717.813,	98.829,	0.000,	-693.106,	98.829,	-0.000
166.000,	-722.085,	98.829,	0.000,	-697.378,	98.829,	-0.000
167.000,	-726.356,	98.829,	0.000,	-701.650,	98.829,	-0.000
168.000,	-730.628,	98.829,	0.000,	-705.922,	98.829,	-0.000
169.000,	-734.900,	98.829,	0.000,	-710.193,	98.829,	-0.000
170.000,	-739.172,	98.829,	0.000,	-714.465,	98.829,	-0.000
171.000,	-743.443,	98.829,	0.000,	-718.737,	98.829,	-0.000
172.000,	-747.715,	98.829,	0.000,	-723.009,	98.829,	-0.000
173.000,	-751.987,	98.829,	0.000,	-727.280,	98.829,	-0.000
174.000,	-756.258,	98.829,	0.000,	-731.552,	98.829,	-0.000
175.000,	-760.530,	98.829,	0.000,	-735.824,	98.829,	-0.000
176.000,	-764.802,	98.829,	0.000,	-740.095,	98.829,	-0.000
177.000,	-769.074,	98.829,	0.000,	-744.367,	98.829,	-0.000
178.000,	-773.345,	98.829,	0.000,	-748.639,	98.829,	-0.000
179.000,	-777.617,	98.829,	0.000,	-752.911,	98.829,	-0.000

APA.OUT for TEST CASE #2

yz = 0.000000e+00 zz = 5.000000e+01 vz = 1.723000e+00 bz = 2.984500e+01
zimfac = 1.500000e+00 zgefacc = 6.000000e-01 gamfac = 4.000000e-01 gerfac = 4.000000e-01
geang = 4.500000e+01
t1 = 0.000000e+00 t2 = 1.800000e+02 Nt = 181
t1_img = 0.000000e+00 t2_img = 1.200000e+02 Nt_img = 121
T1_ge1 = 0.000000e+00 T2_ge1 = 1.200000e+02 Nt_ge1 = 121
T1_ge2 = 0.000000e+00 T2_ge2 = 1.200000e+02 Nt_ge2 = 121
kmax = 4000 Dtfac = 1.000000e-02 Eps = 1.000000e-06 H1 = 1.000000e-02
Hmin = 1.000000e-10

GAMMA ROTATION DECAY

ANGLE	FACTOR
0.00000	0.50000
15.00000	0.66667
30.00000	0.83333
45.00000	1.00000
60.00000	0.91667
75.00001	0.83333
90.00000	0.75000
105.00001	0.66667
120.00000	0.58333
135.00000	0.50000
150.00001	0.41667
165.00001	0.33333
180.00001	0.25000
195.00000	0.16667
210.00001	0.08333
225.00000	0.00000
240.00001	0.00000
255.00000	0.00000
270.00000	0.00000
285.00000	0.00000
300.00002	0.00000
315.00002	0.00000
330.00002	0.16667
344.99999	0.33333
360.00001	0.50000

Index Height Temperature

0	0.50000	24.11000
1	1.65000	23.87000
2	3.05000	23.76000
3	4.74000	23.67000
4	6.78000	23.60000
5	9.25000	23.54000
6	12.24000	23.47000
7	15.85000	23.41000
8	20.22000	23.35000
9	25.51000	23.28000
10	31.90000	23.20000
11	39.63000	23.11000
12	48.98000	23.02000
13	60.29000	22.90000
14	73.97000	22.93000

15	90.51000	23.20000
16	110.52000	23.60000
17	134.71001	24.24000
18	163.97000	25.33000
19	199.36000	25.12000
20	242.17000	25.07000
21	293.94000	25.50000
22	353.94000	26.28000
23	413.94000	26.51000
24	473.94000	26.28000
25	533.94000	25.71000
26	593.94000	25.15000
27	653.94000	24.64000
28	713.94000	24.42000
29	773.94000	23.92000
30	833.94000	23.42000
31	893.94000	23.25000
32	953.94000	22.78000
33	1013.94000	22.26000
34	1073.93994	21.97000
35	1133.93994	21.55000
36	1193.93994	21.09000
37	1253.93994	20.56000
38	1313.93994	20.12000
39	1373.93994	19.57000

 Index Height Cross-Wind

0	0.00000	-2.26000
1	5.00000	-3.70000
2	10.00000	-3.84000
3	15.00000	-4.17000
4	30.00000	-4.25000
5	45.00000	-4.26000
6	60.00000	-4.33000
7	100.00000	-4.27000
8	150.00000	-4.31000
9	200.00000	-4.26000
10	250.00000	-4.48000
11	300.00000	-4.80000
12	350.00000	-5.44000
13	400.00000	-5.88000
14	450.00000	-5.71000
15	500.00000	-5.52000
16	550.00000	-5.78000
17	600.00000	-5.97000

 Index Height EDR TKE

0	0.00000	0.00020	0.10000
1	1000.00000	0.00020	0.10000

**** Separation History ****

t_sep,gam =

0.000000	29.844999	-323.099854
1.000000	29.795235	-320.308929
2.000000	29.744768	-317.539948
3.000000	29.693586	-314.794067
4.000000	29.641678	-312.070984

Initial DGMDT = 2.72308
 DGAM = 2.72308 -2.72308 2.72308
 vz = 1.723000e+00 zim = 4.476750e+01 zge = 1.778501e+01
 gerad = 1.185667e+01 gamfac = 4.000000e-01 zdown = 8.383933e+00 yover = 8.383933e+00

TRAJEC.DAT for TEST CASE #2

TIME	LY	LZ	LCIRC	RY	RZ	RCIRC
0.000,	-14.922,	50.000,	-323.100,	14.922,	50.000,	323.100
1.000,	-19.177,	48.283,	-320.309,	10.618,	48.283,	320.309
2.000,	-23.423,	46.578,	-317.540,	6.322,	46.578,	317.540
3.000,	-27.661,	44.885,	-314.794,	2.033,	44.885,	314.794
4.000,	-31.894,	43.203,	-312.071,	-2.253,	43.203,	312.071
5.067,	-36.506,	41.619,	-309.166,	-6.727,	41.619,	309.166
6.134,	-41.124,	40.072,	-306.261,	-11.193,	40.072,	306.261
7.201,	-45.749,	38.561,	-303.356,	-15.649,	38.561,	303.356
8.267,	-50.388,	37.104,	-300.451,	-20.088,	37.104,	300.451
9.334,	-55.043,	35.700,	-297.546,	-24.508,	35.700,	297.546
10.401,	-59.699,	34.295,	-294.640,	-28.928,	34.295,	294.640
11.468,	-64.354,	32.891,	-291.735,	-33.348,	32.891,	291.735
12.535,	-69.041,	31.603,	-288.830,	-37.732,	31.603,	288.830
13.602,	-73.736,	30.345,	-285.925,	-42.107,	30.345,	285.925
14.668,	-78.452,	29.160,	-283.020,	-46.451,	29.160,	283.020
15.735,	-83.178,	28.009,	-280.115,	-50.779,	28.009,	280.115
16.802,	-87.945,	26.969,	-277.210,	-55.042,	26.969,	277.210
17.869,	-92.726,	25.962,	-274.305,	-59.284,	25.962,	274.305
18.936,	-97.506,	24.956,	-271.400,	-63.526,	24.956,	271.400
20.003,	-102.314,	24.014,	-268.495,	-67.728,	24.014,	268.495
21.069,	-107.183,	23.207,	-265.589,	-71.847,	23.207,	265.589
22.136,	-112.051,	22.399,	-262.684,	-75.967,	22.399,	262.684
23.203,	-116.933,	21.614,	-259.779,	-80.070,	21.614,	259.779
24.270,	-121.903,	20.986,	-256.874,	-84.062,	20.986,	256.874
25.337,	-126.874,	20.357,	-253.969,	-88.054,	20.357,	253.969
26.404,	-131.862,	19.753,	-251.064,	-92.026,	19.753,	251.064
27.470,	-136.932,	19.271,	-248.159,	-95.900,	19.271,	248.159
28.537,	-142.002,	18.789,	-245.254,	-99.775,	18.789,	245.254
29.604,	-147.114,	18.361,	-242.349,	-103.602,	18.361,	242.349
30.671,	-152.271,	17.991,	-239.444,	-107.377,	17.991,	239.444
31.738,	-157.428,	17.621,	-236.538,	-111.152,	17.621,	236.538
32.865,	-162.967,	17.268,	-233.470,	-115.028,	17.256,	233.470
33.992,	-168.647,	16.915,	-230.401,	-118.691,	16.902,	230.401
35.119,	-174.489,	16.628,	-227.332,	-122.113,	16.728,	227.332
36.246,	-180.473,	16.469,	-224.263,	-125.418,	16.862,	224.263
37.373,	-186.558,	16.492,	-221.194,	-128.748,	17.329,	221.194
38.500,	-192.690,	16.729,	-218.125,	-132.225,	18.041,	218.125
39.627,	-198.812,	17.193,	-215.056,	-135.907,	18.827,	215.056
40.754,	-204.873,	17.906,	-211.987,	-139.781,	19.641,	211.987
41.881,	-210.764,	18.769,	-208.918,	-143.842,	20.454,	208.918
43.008,	-216.419,	19.695,	-205.849,	-148.083,	21.226,	205.849
44.135,	-221.826,	20.619,	-202.780,	-152.487,	21.930,	202.780
45.262,	-227.008,	21.489,	-199.712,	-157.028,	22.542,	199.712
46.389,	-231.986,	22.253,	-196.643,	-161.681,	23.035,	196.643
47.516,	-236.809,	22.866,	-193.574,	-166.408,	23.389,	193.574
48.516,	-241.053,	23.211,	-190.851,	-170.573,	23.534,	190.851
49.516,	-245.350,	23.376,	-188.128,	-174.623,	23.531,	188.128

50.516,	-249.743,	23.412,	-185.404,	-178.514,	23.455,	185.404
51.516,	-254.270,	23.366,	-182.681,	-182.226,	23.385,	182.681
52.516,	-258.962,	23.300,	-179.958,	-185.773,	23.403,	179.958
53.516,	-263.809,	23.275,	-177.235,	-189.207,	23.552,	177.235
54.516,	-268.809,	23.361,	-174.512,	-192.562,	23.876,	174.512
55.516,	-273.900,	23.597,	-171.789,	-195.929,	24.350,	171.789
56.516,	-278.982,	23.948,	-169.066,	-199.374,	24.913,	169.066
57.516,	-284.030,	24.408,	-166.343,	-202.926,	25.503,	166.343
58.516,	-289.016,	24.945,	-163.620,	-206.581,	26.107,	163.620
59.516,	-293.911,	25.514,	-160.897,	-210.337,	26.712,	160.897
60.516,	-298.721,	26.098,	-158.174,	-214.184,	27.305,	158.174
61.516,	-303.434,	26.686,	-155.451,	-218.127,	27.874,	155.451
62.516,	-308.064,	27.268,	-152.728,	-222.147,	28.413,	152.728
63.516,	-312.628,	27.823,	-150.004,	-226.225,	28.904,	150.004
64.516,	-317.146,	28.332,	-147.281,	-230.333,	29.328,	147.281
65.516,	-321.621,	28.796,	-144.558,	-234.462,	29.689,	144.558
66.516,	-326.063,	29.220,	-141.835,	-238.602,	29.999,	141.835
67.516,	-330.476,	29.602,	-139.112,	-242.744,	30.261,	139.112
68.516,	-334.864,	29.944,	-136.389,	-246.883,	30.482,	136.389
69.516,	-339.229,	30.243,	-133.666,	-251.016,	30.664,	133.666
70.516,	-343.578,	30.500,	-130.943,	-255.135,	30.812,	130.943
71.516,	-347.920,	30.713,	-128.220,	-259.234,	30.930,	128.220
72.516,	-352.263,	30.883,	-125.497,	-263.305,	31.024,	125.497
73.516,	-356.616,	31.012,	-122.774,	-267.343,	31.103,	122.774
74.516,	-360.987,	31.105,	-120.051,	-271.343,	31.175,	120.051
75.516,	-365.384,	31.171,	-117.327,	-275.305,	31.252,	117.327
76.516,	-369.815,	31.214,	-114.604,	-279.227,	31.344,	114.604
77.516,	-374.282,	31.247,	-111.881,	-283.116,	31.463,	111.881
78.516,	-378.786,	31.279,	-109.158,	-286.981,	31.615,	109.158
79.516,	-383.327,	31.322,	-106.435,	-290.840,	31.798,	106.435
80.516,	-387.902,	31.386,	-103.712,	-294.712,	31.999,	103.712
81.516,	-392.503,	31.478,	-100.989,	-298.602,	32.212,	100.989
82.516,	-397.112,	31.594,	-98.266,	-302.511,	32.432,	98.266
83.516,	-401.714,	31.722,	-95.543,	-306.442,	32.653,	95.543
84.516,	-406.305,	31.859,	-92.820,	-310.393,	32.873,	92.820
85.516,	-410.884,	32.005,	-90.097,	-314.364,	33.092,	90.097
86.516,	-415.452,	32.159,	-87.374,	-318.353,	33.308,	87.374
87.516,	-420.008,	32.318,	-84.650,	-322.359,	33.521,	84.650
88.516,	-424.552,	32.483,	-81.927,	-326.383,	33.730,	81.927
89.516,	-429.085,	32.653,	-79.204,	-330.422,	33.934,	79.204
90.516,	-433.604,	32.824,	-76.481,	-334.475,	34.134,	76.481
91.516,	-438.110,	32.993,	-73.758,	-338.542,	34.328,	73.758
92.516,	-442.600,	33.159,	-71.035,	-342.624,	34.516,	71.035
93.516,	-447.076,	33.324,	-68.312,	-346.710,	34.688,	68.312
94.516,	-451.542,	33.485,	-65.589,	-350.798,	34.850,	65.589
95.516,	-455.997,	33.644,	-62.866,	-354.888,	35.001,	62.866
96.516,	-460.436,	33.798,	-60.143,	-358.981,	35.141,	60.143
97.516,	-464.871,	33.951,	-57.420,	-363.075,	35.277,	57.420
98.516,	-469.290,	34.090,	-54.697,	-367.174,	35.403,	54.697
99.516,	-473.708,	34.227,	-51.973,	-371.274,	35.528,	51.973
100.516,	-478.116,	34.350,	-49.250,	-375.381,	35.645,	49.250
101.516,	-482.524,	34.473,	-46.527,	-379.487,	35.762,	46.527
102.516,	-486.918,	34.579,	-43.804,	-383.605,	35.871,	43.804
103.516,	-491.312,	34.686,	-41.081,	-387.722,	35.979,	41.081
104.516,	-495.696,	34.784,	-38.358,	-391.849,	36.081,	38.358
105.516,	-500.073,	34.876,	-35.635,	-395.982,	36.179,	35.635
106.516,	-504.450,	34.968,	-32.912,	-400.115,	36.277,	32.912
107.516,	-508.809,	35.046,	-30.189,	-404.264,	36.364,	30.189
108.516,	-513.165,	35.121,	-27.466,	-408.418,	36.448,	27.466
109.516,	-517.520,	35.196,	-24.743,	-412.571,	36.532,	24.743
110.516,	-521.857,	35.258,	-22.020,	-416.742,	36.603,	22.020
111.516,	-526.187,	35.314,	-19.296,	-420.920,	36.669,	19.296

112.516,	-530.517,	35.370,	-16.573,	-425.098,	36.735,	16.573
113.516,	-534.840,	35.422,	-13.850,	-429.283,	36.795,	13.850
114.516,	-539.140,	35.456,	-11.127,	-433.490,	36.837,	11.127
115.516,	-543.440,	35.490,	-8.404,	-437.698,	36.878,	8.404
116.516,	-547.740,	35.525,	-5.681,	-441.906,	36.920,	5.681
117.516,	-552.033,	35.554,	-3.361,	-446.121,	36.955,	3.361
118.516,	-556.298,	35.562,	-2.569,	-450.364,	36.965,	2.569
119.516,	-560.563,	35.570,	-1.777,	-454.607,	36.976,	1.777
120.516,	-564.828,	35.579,	-0.985,	-458.850,	36.986,	0.985
121.516,	-569.093,	35.587,	-0.193,	-463.093,	36.996,	0.193
122.516,	-573.349,	35.589,	0.000,	-467.345,	36.999,	0.000
123.516,	-577.603,	35.589,	0.000,	-471.600,	36.999,	0.000
124.516,	-581.857,	35.589,	0.000,	-475.854,	36.999,	0.000
125.516,	-586.110,	35.589,	0.000,	-480.109,	36.999,	0.000
126.516,	-590.364,	35.589,	0.000,	-484.364,	36.999,	0.000
127.516,	-594.618,	35.589,	0.000,	-488.618,	36.999,	0.000
128.516,	-598.872,	35.589,	0.000,	-492.873,	36.999,	0.000
129.516,	-603.125,	35.589,	0.000,	-497.128,	36.999,	0.000
130.516,	-607.379,	35.589,	0.000,	-501.382,	36.999,	0.000
131.516,	-611.633,	35.589,	0.000,	-505.637,	36.999,	0.000
132.516,	-615.886,	35.589,	0.000,	-509.892,	36.999,	0.000
133.516,	-620.140,	35.589,	0.000,	-514.146,	36.999,	0.000
134.516,	-624.394,	35.589,	0.000,	-518.401,	36.999,	0.000
135.516,	-628.648,	35.589,	0.000,	-522.656,	36.999,	0.000
136.516,	-632.901,	35.589,	0.000,	-526.910,	36.999,	0.000
137.516,	-637.155,	35.589,	0.000,	-531.165,	36.999,	0.000
138.516,	-641.409,	35.589,	0.000,	-535.420,	36.999,	0.000
139.516,	-645.663,	35.589,	0.000,	-539.674,	36.999,	0.000
140.516,	-649.916,	35.589,	0.000,	-543.929,	36.999,	0.000
141.516,	-654.170,	35.589,	0.000,	-548.184,	36.999,	0.000
142.516,	-658.424,	35.589,	0.000,	-552.438,	36.999,	0.000
143.516,	-662.677,	35.589,	0.000,	-556.693,	36.999,	0.000
144.516,	-666.931,	35.589,	0.000,	-560.948,	36.999,	0.000
145.516,	-671.185,	35.589,	0.000,	-565.202,	36.999,	0.000
146.516,	-675.439,	35.589,	0.000,	-569.457,	36.999,	0.000
147.516,	-679.692,	35.589,	0.000,	-573.712,	36.999,	0.000
148.516,	-683.946,	35.589,	0.000,	-577.966,	36.999,	0.000
149.516,	-688.200,	35.589,	0.000,	-582.221,	36.999,	0.000
150.516,	-692.453,	35.589,	0.000,	-586.476,	36.999,	0.000
151.516,	-696.707,	35.589,	0.000,	-590.730,	36.999,	0.000
152.516,	-700.961,	35.589,	0.000,	-594.985,	36.999,	0.000
153.516,	-705.215,	35.589,	0.000,	-599.240,	36.999,	0.000
154.516,	-709.468,	35.589,	0.000,	-603.494,	36.999,	0.000
155.516,	-713.722,	35.589,	0.000,	-607.749,	36.999,	0.000
156.516,	-717.976,	35.589,	0.000,	-612.004,	36.999,	0.000
157.516,	-722.230,	35.589,	0.000,	-616.258,	36.999,	0.000
158.516,	-726.483,	35.589,	0.000,	-620.513,	36.999,	0.000
159.516,	-730.737,	35.589,	0.000,	-624.768,	36.999,	0.000
160.516,	-734.991,	35.589,	0.000,	-629.022,	36.999,	0.000
161.516,	-739.245,	35.589,	0.000,	-633.277,	36.999,	0.000
162.516,	-743.498,	35.589,	0.000,	-637.532,	36.999,	0.000
163.516,	-747.752,	35.589,	0.000,	-641.786,	36.999,	0.000
164.516,	-752.006,	35.589,	0.000,	-646.041,	36.999,	0.000
165.516,	-756.259,	35.589,	0.000,	-650.296,	36.999,	0.000
166.516,	-760.513,	35.589,	0.000,	-654.550,	36.999,	0.000
167.516,	-764.767,	35.589,	0.000,	-658.805,	36.999,	0.000

APA.OUT for TEST CASE #3

yz = 0.000000e+00 zz = 2.500000e+01 vz = 1.723000e+00 bz = 2.984500e+01
zimfac = 1.500000e+00 zgefacc = 6.000000e-01 gamfac = 4.000000e-01 gerfac = 4.000000e-01
geang = 4.500000e+01
t1 = 0.000000e+00 t2 = 1.800000e+02 Nt = 181
t1_img = 0.000000e+00 t2_img = 1.200000e+02 Nt_img = 121
T1_ge1 = 0.000000e+00 T2_ge1 = 1.200000e+02 Nt_ge1 = 121
T1_ge2 = 0.000000e+00 T2_ge2 = 1.200000e+02 Nt_ge2 = 121
kmax = 4000 Dtfac = 1.000000e-02 Eps = 1.000000e-06 H1 = 1.000000e-02
Hmin = 1.000000e-10

GAMMA ROTATION DECAY

ANGLE	FACTOR
0.00000	0.50000
15.00000	0.66667
30.00000	0.83333
45.00000	1.00000
60.00000	0.91667
75.00001	0.83333
90.00000	0.75000
105.00001	0.66667
120.00000	0.58333
135.00000	0.50000
150.00001	0.41667
165.00001	0.33333
180.00001	0.25000
195.00000	0.16667
210.00001	0.08333
225.00000	0.00000
240.00001	0.00000
255.00000	0.00000
270.00000	0.00000
285.00000	0.00000
300.00002	0.00000
315.00002	0.00000
330.00002	0.16667
344.99999	0.33333
360.00001	0.50000

Index	Height	Temperature
-------	--------	-------------

0	0.50000	24.11000
1	1.65000	23.87000
2	3.05000	23.76000
3	4.74000	23.67000
4	6.78000	23.60000
5	9.25000	23.54000
6	12.24000	23.47000
7	15.85000	23.41000
8	20.22000	23.35000
9	25.51000	23.28000
10	31.90000	23.20000
11	39.63000	23.11000
12	48.98000	23.02000
13	60.29000	22.90000

14	73.97000	22.93000
15	90.51000	23.20000
16	110.52000	23.60000
17	134.71001	24.24000
18	163.97000	25.33000
19	199.36000	25.12000
20	242.17000	25.07000
21	293.94000	25.50000
22	353.94000	26.28000
23	413.94000	26.51000
24	473.94000	26.28000
25	533.94000	25.71000
26	593.94000	25.15000
27	653.94000	24.64000
28	713.94000	24.42000
29	773.94000	23.92000
30	833.94000	23.42000
31	893.94000	23.25000
32	953.94000	22.78000
33	1013.94000	22.26000
34	1073.93994	21.97000
35	1133.93994	21.55000
36	1193.93994	21.09000
37	1253.93994	20.56000
38	1313.93994	20.12000
39	1373.93994	19.57000

Index	Height	Cross-Wind
0	0.00000	-2.26000
1	5.00000	-3.70000
2	10.00000	-3.84000
3	15.00000	-4.17000
4	30.00000	-4.25000
5	45.00000	-4.26000
6	60.00000	-4.33000
7	100.00000	-4.27000
8	150.00000	-4.31000
9	200.00000	-4.26000
10	250.00000	-4.48000
11	300.00000	-4.80000
12	350.00000	-5.44000
13	400.00000	-5.88000
14	450.00000	-5.71000
15	500.00000	-5.52000
16	550.00000	-5.78000
17	600.00000	-5.97000

Index	Height	EDR	TKE
0	0.00000	0.00020	0.10000
1	1000.00000	0.00020	0.10000

***** Separation History *****

t,sep,gam =
 0.000000 29.844999 -323.099854
 1.000000 29.795235 -320.309265

Initial DGMDT = 2.79059
 DGAM = 2.79059 -2.79059 -2.79059 2.79059
 vz = 1.723000e+00 zim = 2.475000e+01 zge = 1.787714e+01
 gerad = 1.191809e+01 gamfac = 4.000000e-01 zdown = 8.427365e+00 yover = 8.427365e+00

14.731, -89.785, 17.361, -281.991, -34.503, 18.879, 281.991

TRAJEC.DAT for TEST CASE #3

TIME	LY	LZ	LCIRC	RY	RZ	RCIRC
0.000,	-14.922,	25.000,	-323.100,	14.922,	25.000,	323.100
1.000,	-19.116,	23.283,	-320.309,	10.679,	23.283,	320.309
2.230,	-24.729,	21.860,	-316.876,	5.933,	21.860,	316.876
3.460,	-30.416,	20.572,	-313.443,	1.279,	20.572,	313.443
4.691,	-36.186,	19.422,	-310.010,	-3.277,	19.422,	310.010
5.921,	-42.047,	18.407,	-306.577,	-7.728,	18.407,	306.577
7.151,	-48.011,	17.528,	-303.144,	-12.064,	17.528,	303.144
8.234,	-53.412,	16.828,	-300.122,	-15.701,	16.813,	300.122
9.317,	-59.060,	16.197,	-297.100,	-18.996,	16.192,	297.100
10.400,	-64.983,	15.743,	-294.078,	-21.941,	15.932,	294.078
11.483,	-71.128,	15.570,	-291.056,	-24.764,	16.196,	291.056
12.566,	-77.407,	15.767,	-288.035,	-27.703,	16.948,	288.035
13.648,	-83.684,	16.387,	-285.013,	-30.949,	17.884,	285.013
15.814,	-95.524,	18.493,	-278.969,	-38.368,	19.848,	278.969
16.897,	-100.849,	19.626,	-275.947,	-42.514,	20.702,	275.947
17.980,	-105.790,	20.628,	-272.925,	-46.892,	21.373,	272.925
19.063,	-110.441,	21.386,	-269.904,	-51.416,	21.803,	269.904
20.063,	-114.677,	21.717,	-267.113,	-55.530,	21.882,	267.113
21.063,	-119.070,	21.729,	-264.322,	-59.365,	21.726,	264.322
22.063,	-123.763,	21.567,	-261.532,	-62.813,	21.563,	261.532
23.063,	-128.823,	21.428,	-258.741,	-65.928,	21.630,	258.741
24.063,	-134.216,	21.520,	-255.951,	-68.864,	22.059,	255.951
25.063,	-139.726,	21.907,	-253.160,	-71.864,	22.789,	253.160
26.063,	-145.194,	22.549,	-250.369,	-75.060,	23.637,	250.369
27.063,	-150.514,	23.366,	-247.579,	-78.476,	24.527,	247.579
28.063,	-155.629,	24.246,	-244.788,	-82.105,	25.412,	244.788
29.063,	-160.531,	25.141,	-241.998,	-85.936,	26.250,	241.998
30.063,	-165.268,	25.981,	-239.207,	-89.897,	26.968,	239.207
31.063,	-169.893,	26.709,	-236.417,	-93.914,	27.529,	236.417
32.063,	-174.416,	27.346,	-233.626,	-97.966,	27.971,	233.626
33.063,	-178.856,	27.875,	-230.835,	-102.023,	28.301,	230.835
34.063,	-183.247,	28.274,	-228.045,	-106.041,	28.524,	228.045
35.063,	-187.634,	28.538,	-225.254,	-109.980,	28.665,	225.254
36.063,	-192.068,	28.677,	-222.464,	-113.798,	28.765,	222.464
37.063,	-196.614,	28.720,	-219.673,	-117.458,	28.886,	219.673
38.063,	-201.316,	28.721,	-216.882,	-120.965,	29.114,	216.882
39.063,	-206.177,	28.765,	-214.092,	-124.431,	29.457,	214.092
40.063,	-211.166,	28.921,	-211.301,	-127.937,	29.869,	211.301
41.063,	-216.167,	29.154,	-208.511,	-131.499,	30.320,	208.511
42.063,	-221.153,	29.446,	-205.720,	-135.122,	30.791,	205.720
43.063,	-226.117,	29.794,	-202.929,	-138.804,	31.276,	202.929
44.063,	-231.053,	30.193,	-200.139,	-142.541,	31.767,	200.139
45.063,	-235.949,	30.618,	-197.348,	-146.293,	32.225,	197.348
46.063,	-240.800,	31.065,	-194.558,	-150.020,	32.649,	194.558
47.063,	-245.642,	31.495,	-191.767,	-153.722,	33.076,	191.767
48.063,	-250.502,	31.906,	-188.977,	-157.402,	33.529,	188.977

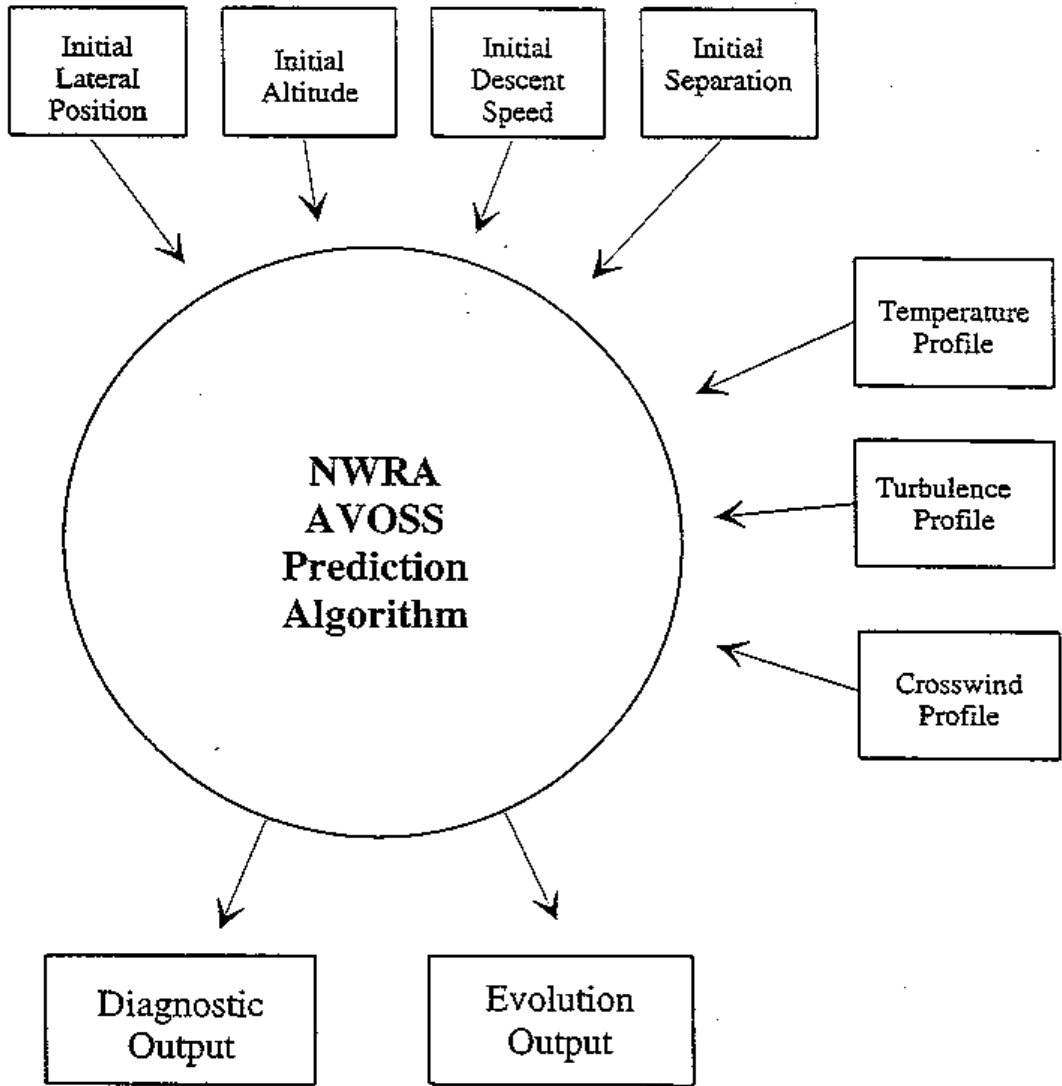
49.063,	-255.378,	32.319,	-186.186,	-161.074,	34.017,	186.186
50.063,	-260.263,	32.750,	-183.395,	-164.749,	34.546,	183.395
51.063,	-265.152,	33.206,	-180.605,	-168.439,	35.117,	180.605
52.063,	-270.037,	33.691,	-177.814,	-172.150,	35.726,	177.814
53.063,	-274.914,	34.204,	-175.024,	-175.887,	36.367,	175.024
54.063,	-279.777,	34.747,	-172.233,	-179.659,	37.036,	172.233
55.063,	-284.620,	35.319,	-169.442,	-183.470,	37.726,	169.442
56.063,	-289.440,	35.914,	-166.652,	-187.319,	38.430,	166.652
57.063,	-294.237,	36.531,	-163.861,	-191.208,	39.142,	163.861
58.063,	-299.001,	37.170,	-161.071,	-195.145,	39.853,	161.071
59.063,	-303.734,	37.822,	-158.280,	-199.125,	40.557,	158.280
60.063,	-308.439,	38.485,	-155.489,	-203.139,	41.250,	155.489
61.063,	-313.114,	39.155,	-152.699,	-207.190,	41.923,	152.699
62.063,	-317.755,	39.827,	-149.908,	-211.286,	42.559,	149.908
63.063,	-322.356,	40.499,	-147.118,	-215.427,	43.141,	147.118
64.063,	-326.926,	41.166,	-144.327,	-219.595,	43.677,	144.327
65.063,	-331.462,	41.825,	-141.536,	-223.787,	44.160,	141.536
66.063,	-335.967,	42.474,	-138.746,	-227.990,	44.595,	138.746
67.063,	-340.439,	43.107,	-135.955,	-232.198,	44.982,	135.955
68.063,	-344.879,	43.719,	-133.165,	-236.401,	45.328,	133.165
69.063,	-349.284,	44.301,	-130.374,	-240.591,	45.639,	130.374
70.063,	-353.657,	44.851,	-127.584,	-244.764,	45.923,	127.584
71.063,	-357.997,	45.362,	-124.793,	-248.909,	46.193,	124.793
72.063,	-362.317,	45.839,	-122.002,	-253.033,	46.465,	122.002
73.063,	-366.617,	46.283,	-119.212,	-257.141,	46.748,	119.212
74.063,	-370.903,	46.692,	-116.421,	-261.255,	47.032,	116.421
75.063,	-375.180,	47.069,	-113.631,	-265.388,	47.305,	113.631
76.063,	-379.449,	47.415,	-110.840,	-269.538,	47.567,	110.840
77.063,	-383.715,	47.733,	-108.049,	-273.705,	47.819,	108.049
78.063,	-387.979,	48.023,	-105.259,	-277.887,	48.060,	105.259
79.063,	-392.245,	48.286,	-102.468,	-282.084,	48.290,	102.468
80.063,	-396.516,	48.526,	-99.678,	-286.295,	48.508,	99.678
81.063,	-400.793,	48.746,	-96.887,	-290.517,	48.716,	96.887
82.063,	-405.077,	48.949,	-94.096,	-294.750,	48.913,	94.096
83.063,	-409.371,	49.139,	-91.306,	-298.991,	49.098,	91.306
84.063,	-413.675,	49.320,	-88.515,	-303.216,	49.254,	88.515
85.063,	-417.992,	49.494,	-85.725,	-307.416,	49.384,	85.725
86.063,	-422.320,	49.666,	-82.934,	-311.596,	49.504,	82.934
87.063,	-426.655,	49.838,	-80.144,	-315.762,	49.619,	80.144
88.063,	-430.998,	50.010,	-77.353,	-319.913,	49.731,	77.353
89.063,	-435.343,	50.182,	-74.562,	-324.048,	49.848,	74.562
90.063,	-439.685,	50.349,	-71.772,	-328.177,	49.970,	71.772
91.063,	-444.022,	50.509,	-68.981,	-332.300,	50.097,	68.981
92.063,	-448.352,	50.659,	-66.191,	-336.421,	50.235,	66.191
93.063,	-452.679,	50.803,	-63.400,	-340.543,	50.379,	63.400
94.063,	-457.002,	50.942,	-60.609,	-344.666,	50.527,	60.609
95.063,	-461.321,	51.070,	-57.819,	-348.797,	50.683,	57.819
96.063,	-465.637,	51.192,	-55.028,	-352.933,	50.841,	55.028
97.063,	-469.950,	51.309,	-52.238,	-357.074,	51.002,	52.238
98.063,	-474.260,	51.416,	-49.447,	-361.227,	51.164,	49.447
99.063,	-478.569,	51.519,	-46.656,	-365.386,	51.326,	46.656
100.063,	-482.875,	51.613,	-43.866,	-369.556,	51.486,	43.866
101.063,	-487.179,	51.702,	-41.075,	-373.735,	51.643,	41.075
102.063,	-491.482,	51.785,	-38.285,	-377.922,	51.796,	38.285
103.063,	-495.784,	51.860,	-35.494,	-382.120,	51.943,	35.494
104.063,	-500.084,	51.931,	-32.704,	-386.325,	52.086,	32.704
105.063,	-504.384,	51.997,	-29.913,	-390.538,	52.222,	29.913
106.063,	-508.682,	52.055,	-27.122,	-394.763,	52.347,	27.122
107.063,	-512.980,	52.112,	-24.332,	-398.987,	52.472,	24.332
108.063,	-517.277,	52.157,	-21.541,	-403.230,	52.575,	21.541
109.063,	-521.574,	52.201,	-18.751,	-407.474,	52.677,	18.751
110.063,	-525.872,	52.236,	-15.960,	-411.728,	52.763,	15.960

111.063,	-530.170,	52.266,	-13.169,	-415.988,	52.839,	13.169
112.063,	-534.468,	52.296,	-10.379,	-420.249,	52.916,	10.379
113.063,	-538.766,	52.313,	-7.588,	-424.524,	52.964,	7.588
114.063,	-543.063,	52.328,	-4.798,	-428.802,	53.009,	4.798
115.063,	-547.361,	52.343,	-2.007,	-433.079,	53.053,	2.007
116.063,	-551.657,	52.348,	-1.089,	-437.371,	53.067,	1.089
117.063,	-555.951,	52.350,	-0.678,	-441.666,	53.073,	0.678
118.063,	-560.246,	52.352,	-0.267,	-445.961,	53.080,	0.267
119.063,	-564.541,	52.353,	0.000,	-450.257,	53.084,	0.000
120.063,	-568.835,	52.353,	0.000,	-454.554,	53.084,	0.000
121.063,	-573.130,	52.353,	0.000,	-458.852,	53.084,	0.000
122.063,	-577.424,	52.353,	0.000,	-463.150,	53.084,	0.000
123.063,	-581.718,	52.353,	0.000,	-467.447,	53.084,	0.000
124.063,	-586.013,	52.353,	0.000,	-471.745,	53.084,	0.000
125.063,	-590.307,	52.353,	0.000,	-476.043,	53.084,	0.000
126.063,	-594.601,	52.353,	0.000,	-480.341,	53.084,	0.000
127.063,	-598.896,	52.353,	0.000,	-484.638,	53.084,	0.000
128.063,	-603.190,	52.353,	0.000,	-488.936,	53.084,	0.000
129.063,	-607.484,	52.353,	0.000,	-493.234,	53.084,	0.000
130.063,	-611.779,	52.353,	0.000,	-497.532,	53.084,	0.000
131.063,	-616.073,	52.353,	0.000,	-501.829,	53.084,	0.000
132.063,	-620.367,	52.353,	0.000,	-506.127,	53.084,	0.000
133.063,	-624.662,	52.353,	0.000,	-510.425,	53.084,	0.000
134.063,	-628.956,	52.353,	0.000,	-514.722,	53.084,	0.000
135.063,	-633.250,	52.353,	0.000,	-519.020,	53.084,	0.000
136.063,	-637.545,	52.353,	0.000,	-523.318,	53.084,	0.000
137.063,	-641.839,	52.353,	0.000,	-527.616,	53.084,	0.000
138.063,	-646.133,	52.353,	0.000,	-531.913,	53.084,	0.000
139.063,	-650.427,	52.353,	0.000,	-536.211,	53.084,	0.000

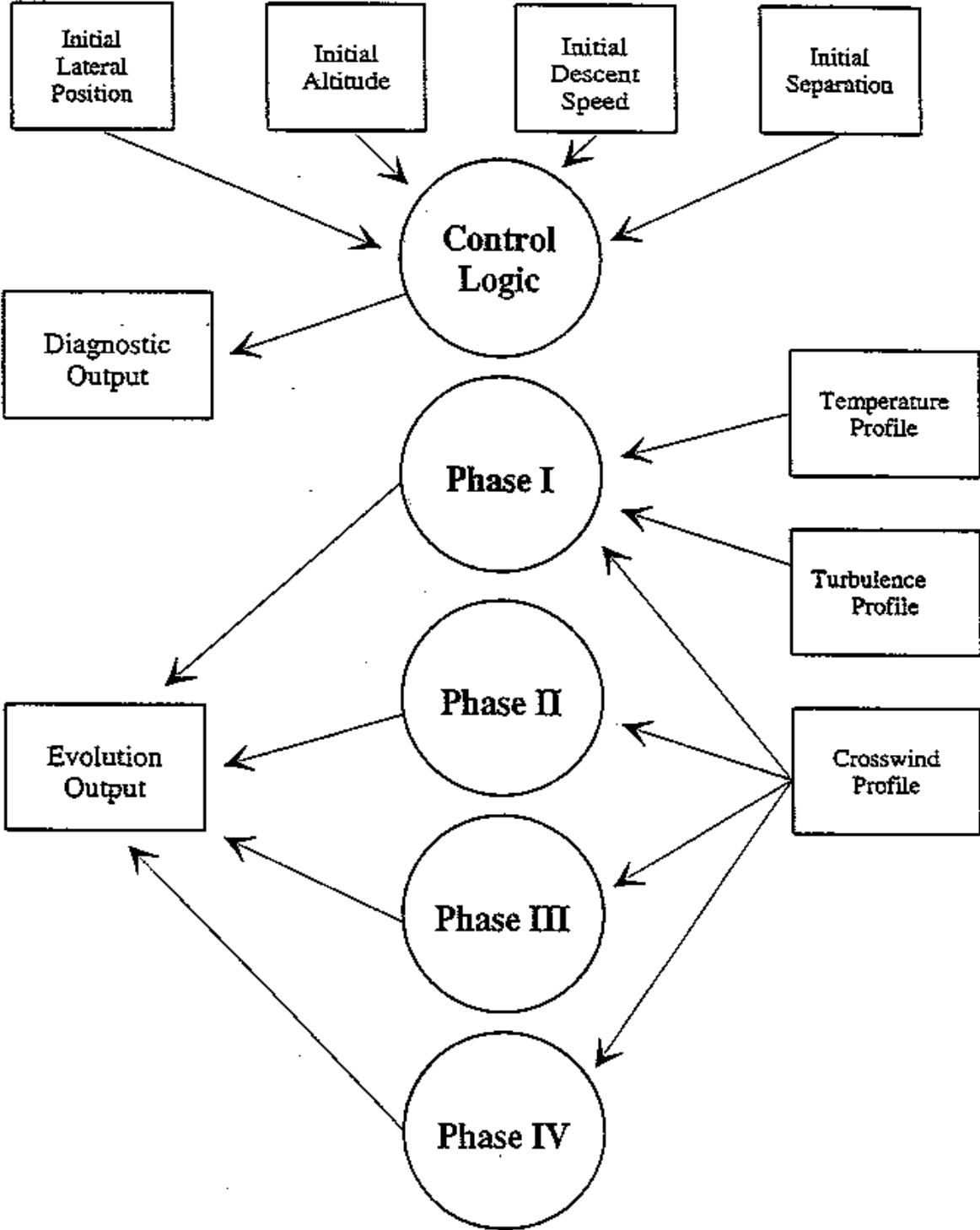
Appendix G. Supplementary Charts

On the following pages are level 0 and level 1 data flow diagrams, and a control flow chart for the prediction algorithm. This information is included to supplement the flow chart presented in Fig. 2.

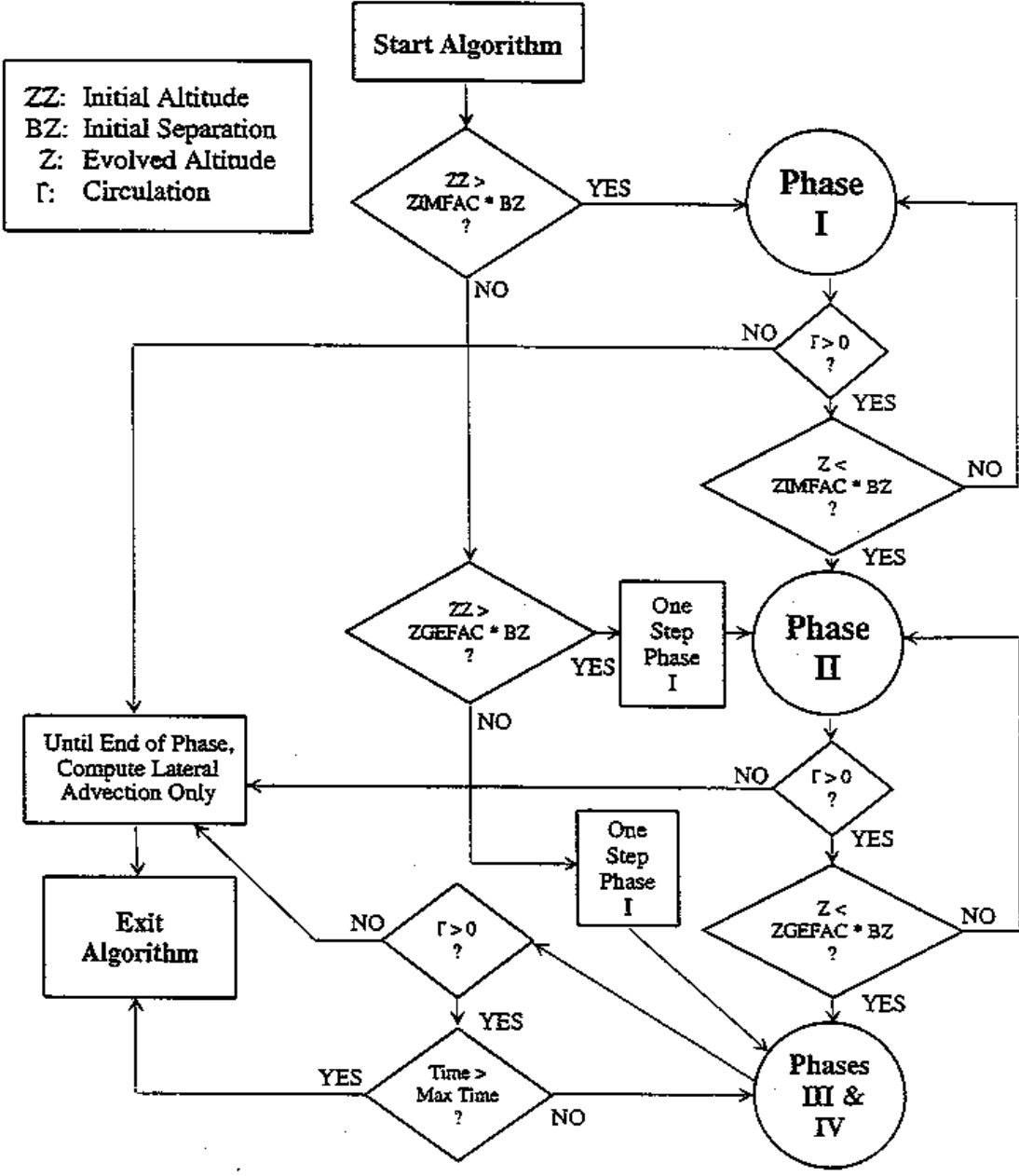
LEVEL 0 DATA FLOW DIAGRAM



LEVEL 1 DATA FLOW DIAGRAM



CONTROL FLOW CHART



REPORT DOCUMENTATION PAGE			Form Approved OMB No. 0704-0188	
Public reporting burden for this collection of information is estimated to average 1 hour per response, including the time for reviewing instructions, searching existing data sources, gathering and maintaining the data needed, and completing and reviewing the collection of information. Send comments regarding this burden estimate or any other aspect of this collection of information, including suggestions for reducing this burden, to Washington Headquarters Services, Directorate for Information Operations and Reports, 1215 Jefferson Davis Highway, Suite 1204, Arlington, VA 22202-4302, and to the Office of Management and Budget, Paperwork Reduction Project (0704-0188), Washington, DC 20503.				
1. AGENCY USE ONLY (Leave blank)		2. REPORT DATE June 2002	3. REPORT TYPE AND DATES COVERED Contractor Report	
4. TITLE AND SUBTITLE NWRA AVOSS Wake Vortex Prediction Algorithm Version 3.1.1			5. FUNDING NUMBERS NAS1-99074	
6. AUTHOR(S) R. E. Robins and D. P. Delisi			727-04-10-01	
7. PERFORMING ORGANIZATION NAME(S) AND ADDRESS(ES) Northwest Research Associates, Inc. 14508 NE 20th Street Bellevue, WA 98007-3713			8. PERFORMING ORGANIZATION REPORT NUMBER NWRA-CR-00-R229A	
9. SPONSORING/MONITORING AGENCY NAME(S) AND ADDRESS(ES) National Aeronautics and Space Administration Langley Research Center Hampton, VA 23681-2199			10. SPONSORING/MONITORING AGENCY REPORT NUMBER NASA/CR-2002-211746	
11. SUPPLEMENTARY NOTES Langley Technical Monitor: David Hinton				
12a. DISTRIBUTION/AVAILABILITY STATEMENT Unclassified-Unlimited Subject Category 3 Distribution: Nonstandard Availability: NASA CASI (301) 621-0390			12b. DISTRIBUTION CODE	
13. ABSTRACT (Maximum 200 words) This report provides a detailed description of the wake vortex prediction algorithm used in the Demonstration Version of NASA's Aircraft Vortex Spacing System (AVOSS). The report includes all equations used in the algorithm, an explanation of how to run the algorithm, and a discussion of how the source code for the algorithm is organized. Several appendices contain important supplementary information, including suggestions for enhancing the algorithm and results from test cases.				
14. SUBJECT TERMS aircraft approach spacing; aircraft wakes; wing tip vortices			15. NUMBER OF PAGES 64	
			16. PRICE CODE	
17. SECURITY CLASSIFICATION OF REPORT Unclassified	18. SECURITY CLASSIFICATION OF THIS PAGE Unclassified	19. SECURITY CLASSIFICATION OF ABSTRACT Unclassified	20. LIMITATION OF ABSTRACT UL	